ATTACHMENT B: AREA OF REVIEW AND CORRECTIVE ACTION PLAN
[40 CFR 146.84(B)]
CTV V

Table of Contents

Document Version History

Version	Revision Date	File Name	Description of Change
1	6/13/2023	Att B - CTV V AoR_CA_v1	Original Submission
2	7/9/2024	Att B - CTV V AoR_CA_v2	Revision in response to EPA comment

1. Facility Information

Facility name: CTV V

Facility contact: William Chessum / Technical Director
(562) 999-8380 / William.chessum@crc.com

Location: CTV V, San Joaquin County, CA
38.08 / -121.42

2. Computational Modeling Approach

The computational modeling workflow begins with the development of a three-dimensional representation of the subsurface geology. It leverages well data (bottom and surface hole location, wellbore trajectory, well logs, etc.) for rendering structural surfaces into a geo-cellular grid, which also includes seismic information to understand faults and flow barriers. Attributes of the grid include porosity, permeability, and facies distributions of reservoir lithologies by subzone, as well as observed fluid contacts and saturations for each fluid phase. This geologic model is often referred to as a static model, as it reflects the reservoir at a single moment. Carbon TerraVault Holdings, LLC (CTV) licenses Schlumberger Petrel, industry-standard geo-cellular modeling software, for building and maintaining static models. The static model becomes dynamic in the computational modeler with the addition of:

- Fluid properties such as density and viscosity for each hydrocarbon and water phase
- Liquid and gas relative permeability
- Capillary pressure data
- Proposed injection well completions, injection rates, and injection pressure over the life of the project
- Field pressure history
- Fluid geochemical analysis

Results from the computational model are used to establish the area of review (AoR), the "region surrounding the geologic sequestration project where underground sources of drinking water (USDWs) may be endangered by the injection activity" [U.S. Environmental Protection Agency (EPA) 75 FR 77230]. In the case of the CTV V storage project, the AoR encompasses the CO_2 plumes and the aerial extent of the critical pressure that would potentially endanger USDWs from brine migration via an open conduit.

2.1 Model Background

Computational modeling was completed using Schlumberger's ECLIPSE 300 (E300) Equation of State Compositional Simulator. E300 is capable of modeling enhanced oil recovery (EOR), chemical EOR, geomechanics, unconventional reservoir, geochemical EOR, and carbon capture and storage. E300 can model flow of three components (gas, oil, and aqueous) and multi-phase

fluids, as well as predict phase equilibrium compositions, densities, and viscosities of each phase. This simulator incorporates all the physics associated with handling of relative permeability as a function of interfacial tension, velocity, composition, and hysteresis. Computational modeling for the carbon dioxide (CO_2) plume used the Peng-Robinson Equation of State. The Peng-Robinson Equation of State establishes the properties of CO_2 over the pressures and temperatures of the model.

The plume model defines the potential quantity of CO_2 stored and simulates lateral and vertical movement of the CO_2 to define the extent of the CO_2 plume and the pressure changes in the reservoir during and after injection which are used to define the AoR.

The simulator predicts the evolution of the CO_2 plume by:

1. Incorporating complex reservoir geometry and wells, and utilizing a full-field, static geological three-dimensional characterization of the reservoir, including lithology, saturation, porosity, and permeability;
2. Forecasting the CO_2 plume movement and growth by inputting the operating parameters into simulation (injection pressure and rates); and
3. Assessing the movement of CO_2 after injection ceases and allowing the plume to reach equilibrium, including pressure equilibrium and compositions in each phase.

Schlumberger's E300 software has been used in numerous CO_2 sequestration peer-reviewed papers, including:

- A Benchmark Study on Problems Related to CO_2 Storage in Geologic Formations (Class et al 2009).
- CO_2 Injectivity, Storage Capacity, Plume Size, and Reservoir and Seal Integrity of the Ordovician St. Peter Sandstone and the Cambrian Potosi Formation in the Illinois Basin (Leetaru et al, 2012).
- Modeling Long Term CO_2 Storage in Saline Aquifers (Mohammed et al., 2012)
- Studying the impact of reservoir temperature, water salinity and CO_2 dryness on CO_2 injectivity during geological CO_2 sequestration (Ahmadi, et al, 2023).
- Probabilistic Risk Assessment of CO_2 Trapping Mechanisms in a Sandstone CO_2-EOR Field in Northern Texas, USA (Jia et al 2016).

2.2 Site Geology and Hydrology

The project involves injecting CO_2 into the Cretaceous-aged Mokelumne River and Starkey formations. Structure in the area is characterized as a homocline that dips about 2 degrees to the southwest. The Mokelumne River Formation is characterized by interbedded shale and sand, while the Starkey Formation contains the Peterson Sandstone Member as its primary sandstone (Upper Confining Zone and Internal Barrier are described in the **Attachment A**). The H&T Shale acts as an Internal Barrier between the Upper and Lower Injection Zones and has an average gross thickness of 146 feet in the Model Boundary. The Capay Shale, which overlies the

Upper Injection zone, serves as the upper confining zone for the project due to its low permeability and thickness. The Capay Shale has an average gross thickness of 500 feet in the Model Boundary and has very low matrix permeability as discussed in section 3.4. Above the Capay Shale are the Domengine Formation and the Nortonville Shale, which serve as the dissipation and an additional barrier, respectively. The Nortonville shale has an average gross thickness of approximately 250 feet within the Model Boundary. The injection zones are present across the entire AoR (**Figure 3.1**). The competence in confining upward fluid movement is established in the Upper Confining Zone by its historical performance as the regional seal for hydrocarbon accumulation in the King Island gas field and nearby gas fields (e.g., River Island, Harte, Sacramento Airport, and Knights Landing). In addition, Pacific Gas and Electric (PG&E) performed an EPA-approved Class V compressed air injection test within the Upper Injection Zone. The test was successful in pressurizing and depressurizing the reservoir without impacting the upper confining zone or bounding Meganos canyon fill.

The Class VI injection wells will target injection in the Mokelumne River (Upper Injection Zone) and Starkey Formation (Lower Injection Zone). Well data, open-hole well logs (**Figure 3.2**), core data, and 2-D and 3-D seismic lines were used to define the subsurface geological characteristics of stratigraphy, lithology, and rock properties. Two normal faults are identified within the project vicinity and model domain. These faults are classified as typical normal faults as seen in the extended area beyond the model domain. Given the typical nature of the faults identified on the seismic data, the lack of major faults mapped by the California Geologic Survey (CGS), and the absence of historical earthquakes within or close to the AoR, the faults identified are not considered to be active or high-risk sources of seismicity and are not considered to be pathways of migration, therefore these faults were not represented as discrete features in the numerical modeling.

2.3 Model Domain

Two separate static geological models, one for the Upper Injection Zone and one for the Lower Injection Zone, were developed using Schlumberger's Petrel software. Petrel is a commonly used software in the petroleum industry for exploration and production. It allows users to incorporate seismic and well data to construct reservoir models and visualize reservoir simulation results. The bottom surface of the Upper Injection Zone model and the top surface of the Lower Injection zone model are consistent between models. Model domain information is summarized in **Table 3.1**.

The static geologic models served as input to the two corresponding simulation models. The Upper Injection Zone geo-cellular and simulation grids used the same Tartan grid, with an average resolution of 494 feet in the x direction and 518 feet in the y direction. The Lower Injection Zone static geologic grid used a uniform geo-cellular grid with a resolution of 250 feet by 250 feet and an average thickness of 19 feet. This grid was used for property distribution. The properties were then upscaled to a Tartan grid for the simulation model, with varying resolutions in the horizontal directions (average of 426 feet in the x direction and average of 487 feet in the y direction), and an average layer thickness of 19 feet. The top four layers in the Lower Injection Zone model are the Internal Barrier, and all underlying layers are part of the Lower Injection Zone. **Figures 3.3a and 3.3b** depict the simulation grids. The model grids are aligned northeast-

southwest (40 degree rotation) parallel to the depositional trend of the injection zones. The lateral model boundaries were generally defined as open boundaries except for three specific boundaries of the lower injection zone. The western boundary of the lower injection zone is designated as a no-flow boundary where the Starkey sand thickness significantly decreases (Downey and Clinkenbeard, 2010). The southeastern boundary of the lower injection zone is set to no-flow where the Starkey sand is truncated by the Stockton arch fault. The northwestern no-flow boundary of the lower injection zone is formed by an unnamed normal fault.

The open-hole logs have a half-foot resolution, and a constant vertical cell height of 19 feet was utilized over the model domain to generate grid layers as shown in **Figure 3.4**. The 19-foot cell height provides the vertical resolution necessary to capture significant lithologic heterogeneity (sand versus shale) which helps to ensure accurate upscaling of log data and distribution of reservoir properties in the static model. **Figure 3.5** shows a comparison of open-hole log data for a well within the AoR and the associated upscaled logs for both the Upper Injection Zone and Lower Injection Zone Models.

2.4 Porosity and Permeability

Wireline log data were acquired with measurements that include but are not limited to spontaneous potential, natural gamma ray, borehole caliper, compressional sonic, resistivity, as well as neutron porosity and bulk density.

Formation porosity is determined from compressional sonic using 55.5 microsecond per foot (μsec/ft) matrix slowness and the Wyllie time average equation (Wyllie et al., 1956). See **Table 3.2** for the Wyllie compaction factors estimated in each zone.

Volume of clay is determined by spontaneous potential and is calibrated to core data. Log-derived permeability is determined by applying a core-based transform that utilizes capillary pressure porosity and permeability along with clay values from x-ray diffraction (XRD) or Fourier-transform infrared spectroscopy (FTIR). Core data from two wells (**Figure 3.6**) with 13 data points were used to develop a permeability transform relating porosity and clay volume to permeability. The transform from core data is illustrated in **Figure 3.7**.

Figure 3.8 shows porosity and permeability histograms for both the Upper Injection Zone and the Lower Injection Zone. Porosity is derived from open-hole well log analysis, and permeability is a function of porosity and clay volume. **Figure 3.9** shows the distribution of permeability and porosity using Sequential Gaussian simulation (kriging) for the Upper Injection Zone and Gaussian Random Function simulation for the Lower Injection Zone within the static model over representative cross sections.

2.5 Constitutive Relationships and Other Rock Properties

Data obtained from cores from the similar geologic age and setting Winters Formation in the neighboring Union Island Gas Field were used for the computational simulation. Based on the representative samples, normalization, averaging, and denormalization of the relative

permeability data was used to generate the gas-water relative permeability curve with endpoints scaling for the computational modeling.

Capillary pressure data are from sidewall core samples taken from the injection zones in well Citizen_Green_1. The simulation and AoR will be updated if additional site-specific data is obtained during the pre-operational testing phase. **Figures 3.10** and **3.11** show the relative permeability curve and capillary pressure curve used in the computational modeling.

2.6 Mineralization

Previous studies into reactive transport modeling and geochemical reaction in CCS have shown that the amount of CO_2 trapped by mineralization reactions is extremely small over a 100-year post injection time frame (Metz et al., 2005) for sandstone reservoirs. For the sake of computational efficiency and the minor expected effect on the AoR, reactive transport was not included as a part of the compositional simulation modeling.

Potential geochemical reactions of the injection zone, confining zone, and formation fluids with the injectate streams being considered were modeled using PHREEQC (ph-REdox-Equilibrium), the USGS geochemical modeling software (USGS, 2019). Details on the modeling procedure and results are provided in **Appendix 3** (CTV V Geochemical Modeling). The modeling indicates as expected that as the formations are stable quartz-dominated mineralogy, the effect of geochemical reactions with the injectate will be minor. Based on molar mass, there is a minimal net molar mass change: 0.2% to 0.5% in the Upper Injection Zone and 0.3% to 0.4% in the Lower Injection Zone. This is not expected to have a major impact on porosity or permeability in the injection zone or upper confining zone.

2.7 Boundary Conditions

The following boundary conditions were applied to the two simulation model domains:

- The Upper Injection Zone model has open-boundary conditions on the west, east, south, and north. Large-volume modifiers were used to model the connection to the reservoir volume beyond the model domain, based on regional mapping of the formations in the area. The top boundary of the model is the overlying shale of the Upper Confining Zone, which was set as a no-flow boundary. The Upper Confining Zone is continuous and present at an average thickness of 500 feet over the model domain. It has low permeability and has been shown to be a proven hydrocarbon seal over the model domain.
- The Lower Injection Zone model has open-boundary conditions on the east, south, and north and no flow boundary conditions on the west, southeast, and northwest. Open boundary conditions were represented by large-volume modifiers to model the connection to the reservoir volume beyond the model domain, based on regional mapping of the formations in the area. The west boundary was set to no-flow where the Starkey sand thins and the southeast and northwest boundaries were set to no-flow based on the presence of faults. The top boundary of the model is the overlying Internal Barrier shale, which was set as a no-flow boundary. The Internal Barrier is continuous and present at an average thickness of 146 feet

over the model domain. It has low permeability and has been shown to be a proven hydrocarbon seal over the model domain.

2.8 Initial Conditions

The initial values of the state variables (pressure, temperature, saturation, and salinity) must be specified throughout the model domain before injection begins. As the initial state is not well-known from direct measurements, a simplified, static distribution is used as an approximation, assuming that the system is initially near equilibrium. Initial model conditions (start of CO_2 injection) of the Upper and Lower Injection Zones are given in **Table 3.3**.

2.9 Operational Information

CTV plans to install six new injectors for the CTV V storage project, with three injectors in the Upper Injection Zone and three injectors in the Lower Injection Zone. The simulations assume a phased injection of 100% CO_2 over 25 years in the Upper Injection Zone and over 15 years in the Lower Injection Zone. Injection rates at the six wells range from 150 kilotons per year (kt/year) to 250 kt/year. Details on the injection operation are presented in **Table 3.4**. Further details are provided in the Narrative document (**Attachment A**) and in the Operational Procedures **Appendix 4**.

2.10 Fracture Pressure and Fracture Gradient

Calculated fracture gradient and target injection pressure values are given in **Table 3.5**. Within the project vicinity, there is a site-specific fracture gradient for the Upper Injection Zone, but not for the Lower Injection Zone or any of the confining zones. A step-rate test will be conducted as per the pre-operational testing plan (**Attachment I**) in the injection zones. A step-rate test was performed in the PG&E TEST_INJECTION_WITHDRAWAL_WELL_1 with a resultant fracture gradient of 0.822 psi/ft in the Upper Injection Zone. Several additional wells in the Sacramento basin have formation integrity tests (FIT) or leak-off tests (LOT) performed at similar depth ranges to the project injection and confining zones. Tests from seven wells average 0.82 psi/ft from tests in the depth range of 4,800 to 11,050 feet TVD. See Figure 2.5-4 of **Attachment A** for location of wells. For the computational simulation modeling and well performance modeling, a fracture gradient of 0.76 psi/ft was assumed for now as a safety factor.

CTV will ensure that the injection pressure is below 90% of the injection zone fracture pressure, calculated at the top of the perforations in the injection wells (**Table 3.5**). CTV expects to operate the wells with a planned downhole injection pressure well below the maximum allowable injection pressure calculated using the fracture gradient and safety factor.

3. Computational Modeling Results

Computational modeling results are provided for the Reference Cases for the Upper and Lower Zones, which provides the basis for delineating the AoR (Section 4.1), and for sensitivity cases that examine the impact of uncertainties in properties on the calculated AoR (Section 4.3).

3.1 Predictions of System Behavior

Figures 4.1 and **Figure 4.2** show the computational modeling results and development of the CO_2 plume at different time steps. The boundaries of the CO_2 plume have been defined with a 1.0 lb-mol/RB CO_2 global net molar density cutoff in the Upper Injection Zone and 0.5 lb-mol/RB CO_2 global net molar density cutoff in the Lower Injection Zone.

A total of 10.3 million metric tons (MMT) CO_2 was estimated to be injected into the Upper Injection Zone and a total of 6.4 MMT was estimated to be injected into the Lower Injection Zone, for a combined total of 16.7 MMT. As shown in **Figure 4.1**, the CO_2 extent is largely defined by 100 years post-injection for the Upper and Lower Injection Zones. The majority of the CO_2 injectate remains as super-critical CO_2 (65% for Upper Injection Zone and 66% for Lower Injection Zone) at the end of the simulation, with the remaining portion of the CO_2 dissolving in the formation brine over the simulated 100 years post injection. **Figure 4.3** shows the cumulative storage for each of the mechanisms.

3.2 Model Calibration and Validation

Model inputs were compared against publicly available reports and presentations by Lawrence Berkley National Laboratory (LBNL) and the West Coast Regional Carbon Sequestration Partnership (WESTCARB) investigating the carbon capture and sequestration (CCS) potential of the area (Foxall et al., 2017; Doughty and Oldenburg, 2011; Beyer et al., 2013). The results of CTV's simulation compare favorably against the previous work by LBNL regarding storage capacity and CO_2 plume size.

3.3 Sensitivity Analysis

Scenarios listed in **Table 4.1** were run to test the effect of varying major model inputs on the CO_2 plume and AoR extent. These scenarios and the comparison against previous work in the area provides us with confidence in the CO_2 plume extent and AoR, and that the corrective action well review and potential impact to the USDWs has been appropriately evaluated.

In addition, the compositional simulation models developed in Schlumberger's E300 software were run for the two simplified injectate compositions discussed in Section 7.2 in **Attachment A**, and their results were also compared against a 100% CO_2 injectate case. The cumulative volume, rate, and injection duration for all three cases were kept the same.

The Upper Injection Zone CO_2 plume for Injectate 1 and Injectate 2 is consistent with the plume outline for 100% CO_2 injectate (**Figure 4.4**), with negligible difference between the three cases. The CO_2 plume outline was defined by a 1.0 global CO_2 net molar density for the Upper Injection Zone for all three cases. The 100-year post-end of injection plumes for the three cases are shown below in **Figure 4.4.** The wells that fall within the CO_2 plume are the same for all three cases. Similarly, the Lower Injection Zone CO_2 plume for Injectate 1 and Injectate 2 is consistent with the plume outline for 100% CO_2 injectate (**Figure 4.4**), and the plume outline was defined by a 0.5 lb-mole/RB global CO_2 net molar density for all three cases. The 100-year

post-end of injection plumes for the three cases are shown below in **Figure 4.4.** The wells that fall within the CO_2 plume are the same for all three cases.

Figure 4.4 shows the Upper Injection Zone and lower injection AoR boundary for the three cases. Additionally, the average pore volume pressure within the project area was plotted for the three cases and was found to be very close, with a maximum difference of ~4 psi seen between the cases for Upper Injection Zone and ~3 psi for the Lower Injection Zone, as shown in **Figure 4.5**. Multiple scenarios were also run to test the effect of mixing Injectate 1 and Injectate 2 in different ratios on the CO_2 plume shapes. As expected, since the resulting mixed injectates were still high-purity CO_2 streams with impurity concentrations in-between those of Injectates 1 and 2, the plume shapes for these scenarios were within the envelope represented by the endpoint compositions.

In summary, there is minimal effect of the minor components on the CO_2 plume shape for the proposed injectate compositions. As such, CTV's plume and AoR modeling for corrective action assessment is adequate for the expected injectate composition ranges. CTV will confirm that the properties of the injectate are consistent with the model inputs at pre-operational injectate sampling and will do so for any additional sources. In addition, the AoR will be reviewed as per Section 6, Reevaluation Schedule and Criteria.

3.4 AoR Delineation

AoR delineation consists of determining the outermost extent of the separate-phase CO_2 plume and area of elevated pressure (pressure front) that pose risk to USDWs during the lifetime of the project. Elevated pressure may pose a risk to USDWs due to the potential for brine leakage from the injection zone into a USDW through a conduit if one is present (e.g., improperly abandoned well). In most cases the AoR will at a minimum be defined by the CO_2 plume footprint and may be larger if the pressure front extends beyond the CO_2 plume. CTV V used the risk based AOR approach as documented in **Appendix 9**.

Various methods are available to determine the pressure threshold value that defines the outermost extent of the pressure front. In general, these methods are used to define a pressure at which brine will leak upwards through an abandoned well, leak into a USDW, and endanger the USDW due to water quality impairment. Risk-based AoR delineation accounts for processes that inhibit brine leakage through abandoned wells (e.g., presence of the mud column) and processes that minimize potential USDW impacts from hypothetical brine leakage (e.g., dilution and attenuation in the USDW). Risk-based AoR delineation strategies are supported by the U.S. EPA (2013) Class VI AoR and Corrective Action Guidance (p. 42).

Appendix 9: Risk Based AoR Delineation includes two reports that document risk-based AoR delineation at CTV V. Risk-based AoR delineation consisted of (1) modeling brine leakage under conservative assumptions and resulting salinity impacts to the lowermost USDW (DBS&A report in **Appendix 9**) and (2) review of wellbore properties in the vicinity of the project and allowable pressure buildup considering the presence of the mud column (Irani Engineering report in **Appendix 9**).

Brine-leakage and USDW salinity transport modeling (DBS&A report in **Appendix 9**) used conservative assumptions and accepted methods to simulate (1) brine leakage through an abandoned well and (2) subsequent contaminant fate and transport within the lowermost USDW. Modeling indicated that the vast majority of brine leakage through a hypothetical abandoned well in the vicinity of the project would discharge to the Domengine dissipation zone (below the lowermost UDSW), and therefore brine leakage to the USDW would be negligible. Concomitantly, elevated salinity levels in the lowermost USDW are calculated to be negligible. These results were based on an assumed injection-zone pressure increase of 500 psi. ECLIPSE modeling results indicate that pressure increase of this magnitude will not occur outside the boundary of the CO_2 plume for both a case considering the CTV V project alone, and a simulation case considering the combined pressure increase from the planned CTV III, CTV V, and Pelican Renewables projects.

Irani Engineering (see **Appendix 9**) has 39 years of experience drilling and completing gas wells in northern California (over 1,000 wells drilled), including reentering five old abandoned wells to assess mud properties. Based on this experience, existing research papers, and third-party reports of reentry into old abandoned wells, they conclude that the modeled pressure increase in the injection zone at the well penetrations in the CTV V project region is not sufficient to induce vertical migration of fluid from the injection zone to the base of the USDW. Specifically, the positive pressure provided by the mud column in the wellbores is well above the modeled pressure increase at these locations due to CO_2 injection. The gel strength of the mud also provides an additional resistance to fluid migration. Gel-based muds used in these abandoned uncased wellbores in the vicinity of CTV V remain in the wellbore, and thus provide resistance to the migration of fluids and will prevent any USDW contamination.

Based on these results pressures great enough to endanger USDWs are not anticipated outside the CO_2 plume footprint, and the final AoR boundary was based on the extent of the CO_2 plume. **Figure 4.8** shows the AoR extent, injector locations, and proposed monitoring well locations. Details on the monitoring wells are discussed further in **Attachment C: Testing and Monitoring Plan**.

4. Corrective Action

4.1 Tabulation of Wells Within the AoR

Wells within the AoR are associated with exploration of the Upper and Lower Injection Zones for natural gas accumulations. Nearby, commercial discoveries of natural gas were developed from 1943 onwards. As such, there are excellent records for wells drilled in the study area, and no undocumented historical wells in the AoR are expected.

CTV accessed internal databases as well as California Geologic Energy Management Division (CalGEM) information to identify and confirm wells within the AoR (CalGEM, 2023a, 2023b).

Table 5.1 provides counts of wellbores that penetrate the upper confining zone within the AoR by status and type for each wellbore with a unique API-12 identifier. **Appendix 6** provides a complete list of all wellbores by API-12 within the AoR. As required by 40 CFR 146.84(c)(2),

the well table in **Appendix 6** describes each well's type, construction, date drilled, location, measured depth, TVD, completion record relative to the Upper and Lower Injection Zones, record of plugging, and requirement for corrective action if necessary. CTV also identified well work to be completed during the pre-operational testing phase.

4.2 Protection of USDWs

For the project area, CTV assessed USDW protection by evaluating all wellbores that penetrate the confining Capay Shale. The corrective action assessment (**Appendix 6**) included the generation a list of existing oil or gas wells within the AoR, the generation of detailed wellbore diagrams for each boring within the CO_2 plumes, review of all perforations, top of cement assessment for each casing string, and determination of cement plug depths. Non-endangerment of USDWs will be ensured during all stages of the project.

4.3 Corrective Action Assessment of Wells in AoR

The depth of the confining zone in each of the wells penetrating the Upper Confining Zone was determined by interpretation of open-hole well logs and utilizing the deviation survey. Six wells in the AoR penetrate the Upper Confining Zone. Two of these wells also penetrate the Internal Barrier. Four previously abandoned wells that penetrate the Upper Confining Zone are within the CO_2 plume boundaries at the corresponding well depths and require reabandonment (corrective action) prior to injection. The remaining wells evaluated do not require any corrective action or are located outside of the AoR (CO_2 plume). Well MCCULLOCH_STEFANI_1 is within the AoR, but does not penetrate the Internal Barrier and the Upper Injection Zone plume is not present at this location. Therefore, MCCULLOCH_STEFANI_1 will not contact the CO_2 plume and no corrective action is required. A map with wells within the AoR is shown in **Figure 5.1**, and the table of wells in **Appendix 6** provides well corrective action assessment pursuant to 40 CFR §146.84(c)(2).

4.4 Plan for Site Access

CTV has obtained surface access rights for the duration of the project.

4.5 Corrective Action Schedule and Procedures

There are four wells within the CO_2 plume boundary that will be reabandoned prior to the start of injection. See **Appendix 7 and Appendix 8** for abandonment procedures and corrective action schematics. CTV will ensure that CO_2 is confined to the injection zones within the AoR, protecting the overlying USDW and ensuring confinement.

Through time, if the plume development is not consistent with the predicted results, computational modeling will be updated to reassess the AoR. In this event, all wells in the updated AoR will be subject to the Corrective Action Plan and be remediated if necessary.

5. Reevaluation Schedule and Criteria

5.1 AoR Reevaluation Cycle

CTV will reevaluate the above described AoR at a minimum every five years during the injection and post-injection phases, as required by 40 CFR 146.84(e).

Simulation study results are reviewed when operating data is acquired. Preparation of necessary operational data for the review includes injection rates and pressures, CO_2 injectate concentrations, and monitoring well information (storage reservoir and overlying dissipation intervals).

Dynamic operating and monitoring data that will be incorporated into future reevaluation will include:

1. Pressure data from monitoring wells that constrain and define plume development.
2. CO_2 content/saturation from monitoring wells. This data may be acquired with direct aqueous measurements and cased-hole log results that will constrain and define plume development.
3. Injection pressures and volumes. The injection pressures and volumes in the computational model are maximum values. If the actual rates are lower than expected, the plume will develop at a slower rate than expected and be reflected in the pressure and CO_2 concentration data in 1 and 2, above.
4. A review of the full suite of water quality data collected from monitoring wells in addition to CO_2 content/saturation (to evaluate the potential for unexpected reactions between the injected fluid and the rock formation).
5. Review and submission of any geologic data acquired since the last modeling effort, including any additional site characterization performed for future injection wells.
6. Reevaluation modeling results will be compared with the most recent modeling (i.e., from the most recent AoR reevaluation). A report describing the comparison of the modeling results will be provided to the EPA with a discussion on whether the results are consistent.
7. Description of the specific actions that will be taken if there are discrepancies between monitoring data and prior modeling results (e.g., remodel the AoR, update all project plans, perform additional corrective action if needed, and submit the results to the EPA).

Reevaluation results will be compared to the original results to understand dynamic inputs affecting plume development and static inputs that would impact injectivity and storage space. Static inputs that may potentially be considered to understand discrepancies between initial and re-evaluation computational models could include permeability, sand continuity and porosity. Although the AoR has been fully delineated, all inputs to the static and dynamic model will be reviewed.

As needed, CTV will review all of the plans that are impacted by a potential AoR increase such as Corrective Action and Emergency and Remedial Response. For corrective action, all wells potentially impacted by a changing AoR will be addressed immediately.

5.2 Triggers for AoR Reevaluations Prior to the Next Scheduled Reevaluation

An ad-hoc re-evaluation prior to the next scheduled re-evaluation will be triggered if any of the following occur:

- Changes in pressure or injection rate that are unexpected and outside three standard deviations from the average
- Difference between the computation modeling and observed plume development:
  - Unexpected changes in fluid constituents or pressure outside the zones of injection that are not related to well integrity
  - Reservoir pressure increase versus injected volume inconsistent with computational modeling results with a variance >±10% from the Base Case Simulation
  - Any other activity prompting a model recalibration
- Seismic monitoring anomalies within two miles of the injection well that are indicative of:
  - The presence of faults near the confining zone that indicates propagation into the confining zone
  - Events reasonably associated with CO_2 injection that are greater than M3.5
- Exceeding 90% of the geologic formation fracture pressure in any injection or monitoring wells
- Detection of changes in shallow groundwater chemistry (e.g., a significant increase in the concentration of any analytical parameter that was not anticipated by the AoR delineation modeling)
- Initiation of competing injection projects within the same injection formation within a 1-mile radius of the injection well (including when additional CTV injection wells come online)
- A significant change in injection operations, as measured by wellhead monitoring
- Significant land-use changes that would impact site access
- Any other activity prompting a model recalibration

CTV will discuss any such events with the UIC Program Director as soon as possible to determine if an AoR re-evaluation is required. If an unscheduled re-evaluation is triggered, CTV will perform the steps described at the beginning of this section of the Plan within six months for the triggering event.

References

Ahmadi, P., F. Ahmaad, M. A. Rahman, S. R. Gomari, 2023. Studying the impact of reservoir temperature, water salinity and CO_2 dryness on CO_2 injectivity during geological CO2 sequestration. Extrica. Advances In Carbon Capture Utilization And Storage. https://www.extrica.com/article/23053/pdf

Beyer, J. H., J. Ajo-Franklin, E. Burton, M. Conrad, C. Doughty, T. Kneafsey, S. Nakagawa, N. Spycher, and M. Voltolini, 2013. *Geologic characterization based on deep core and fluid samples from the Sacramento Basin of California – an Update*. Presented at West Coast Regional Carbon Sequestration Partnership. May 2013.

California Department of Conservation Geologic Energy Management Division (CalGEM). 2023a. Well Statewide Tracking and Reporting System - WellSTAR. https://wellstar.conservation.ca.gov.

California Department of Conservation. Geologic Energy Management Division (CalGEM). 2023b. Online Mapping Application Well Finder. https://maps.conservation.ca.gov/doggr/wellfinder.

Class, H, A. Ebigbo, R. Helmig, H. Dahle, J. Nordbotten, M. Celia, P. Audigane, M. Darcis, J. Ennis-King, Y. Fan, B. Flemisch, S. Gasda, M. Jin, S. Krug, D. Labregere, A. Beni, R. Pawar,

A. Sbai, S. Thomas, L. Trenty, L. Wei, 2009. A benchmark study on problems related to CO2 storage in geologic formations. Comput Geosci. 13:409–434 DOI 10.1007/s10596-009-9146-x.

Downey, C. and J. Clinkenbeard, 2010. Preliminary Geologic Assessment Of The Carbon Sequestration Potentialof The Upper Cretaceous Mokelumne River, Starkey, And Winters Formations – Southern Sacramento Basin, California. Prepared for California Energy Commission and U.S. Department of Energy National Energy Technology Laboratory.

Doughty C., C. Oldenburg. 2011. *Preliminary TOUGH2 model of King Island CO_2 injection*. Presented at West Coast Regional Carbon Sequestration Partnership. October 25, 2011.

Foxall, W., C. Doughty, K. J. Lee, S. Nakagawa, T. Daley, E. Burton, C. Layland-Bachmann, S. Borglin, K. Freeman, J. Ajo-Franklin, P. Jordan, T. Kneafsey, C. Oldenburg, and C. Ulrich, 2017. *Investigation of potential induced seismicity related to Geologic Carbon Dioxide Sequestration in California*. CEC-500-2017-028.

Jia, W., F. Panc, Z. Daid, T. Xiao, M. White, Brian McPherson, 2016. Probabilistic Risk Assessment of CO2 Trapping Mechanisms in a Sandstone CO2-EOR Field in Northern Texas, USA. Energy Procedia, 114: 4321-4329.

Leetaru, H., A. Brown, D. Lee, O. Senel, M. Couëslan, 2012. CO2 Injectivity, Storage Capacity, Plume Size, and Reservoir and Seal Integrity of the Ordovician St. Peter Sandstone and the

Cambrian Potosi Formation in the Illinois Basin. Topical Report. Report Number: DOE/FE0002068-1. U.S. DOE Cooperative Agreement DE-FE0002068.

Metz, B., O. Davidson, H. de Coninck, M. Loos, and L. Meyer (Eds.). *Carbon Dioxide Capture and Storage.* IPCC, 2005. Cambridge University Press, UK. pp. 431. https://www.ipcc.ch/report/carbon-dioxide-capture-and-storage/.

McCutcheon, M.E., D.K. Smith, and G.R. Luther. 1993. *Density and thermal expansion of seawater: Equations of state*. Deep-Sea Research Part II, 40(12), 2211-2223. doi:10.1016/0967-0637(93)90010-V

Mohammed, A., G. Ekoja, A. Adeniyi, A. Hassan. 2012. Modeling long term CO2 storage in saline aquifers. *International Journal of Applied Science and Technology, Vol 2. No. 10*: 53-62

U.S. Geological Survey (USGS). 2019. *User's guide to PHREEQC: A computer program for speciation, batch-reaction, one-dimensional transport, and inverse geochemical calculations*. U.S. Geological Survey Techniques and Methods, book 6, chapter A45. https://pubs.er.usgs.gov/publication/70029490.

Wyllie, M.R.J., D.T. Gregory, and G.H.F. Gardner. 1956. Elasticity of sedimentary rocks. *Journal of Geophysical Research* 61(12): 4189-4216. doi:10.1029/JZ061i012p04189.

Figures

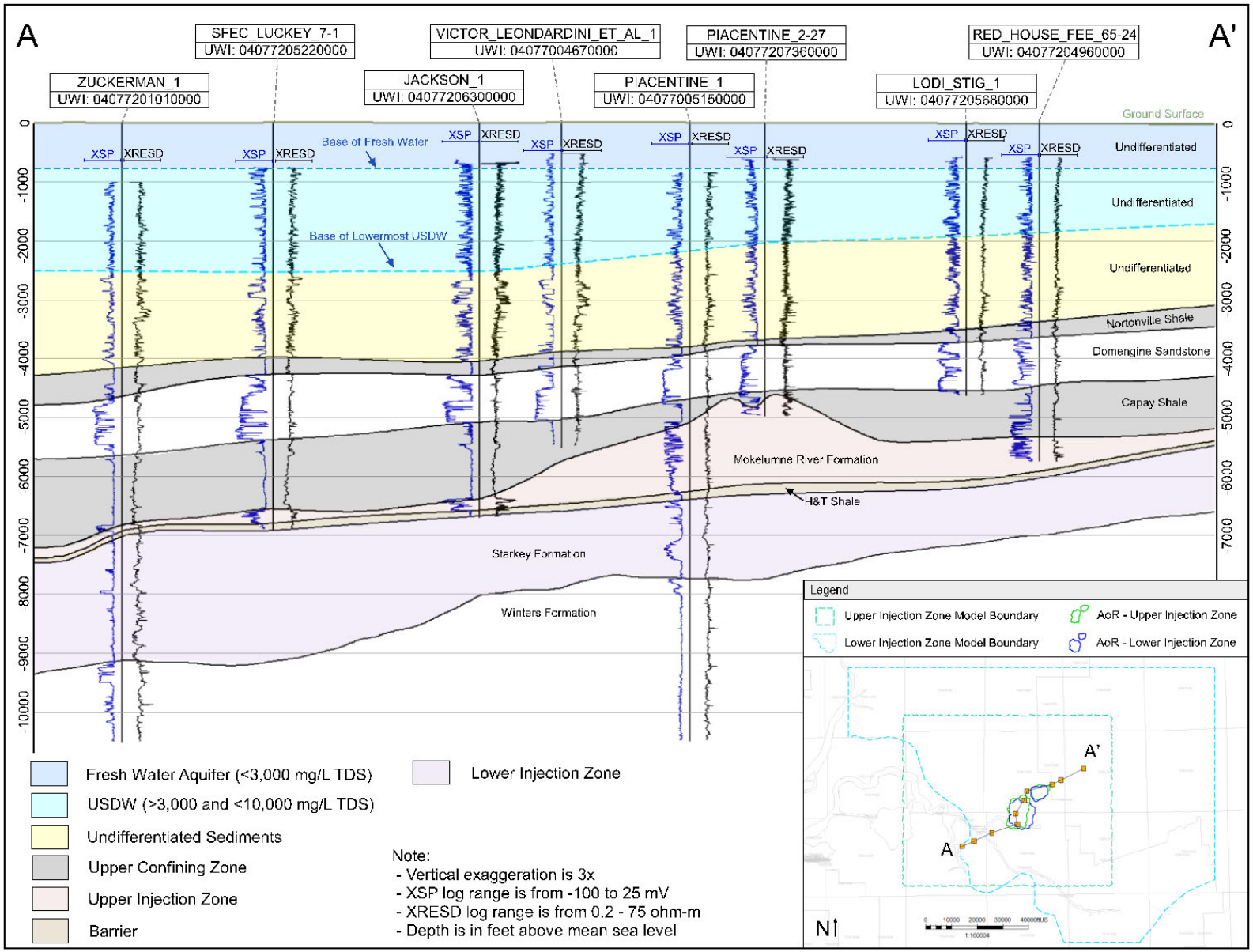

Figure 3.1. Cross section showing stratigraphy and lateral continuity of major formations across the AoR.

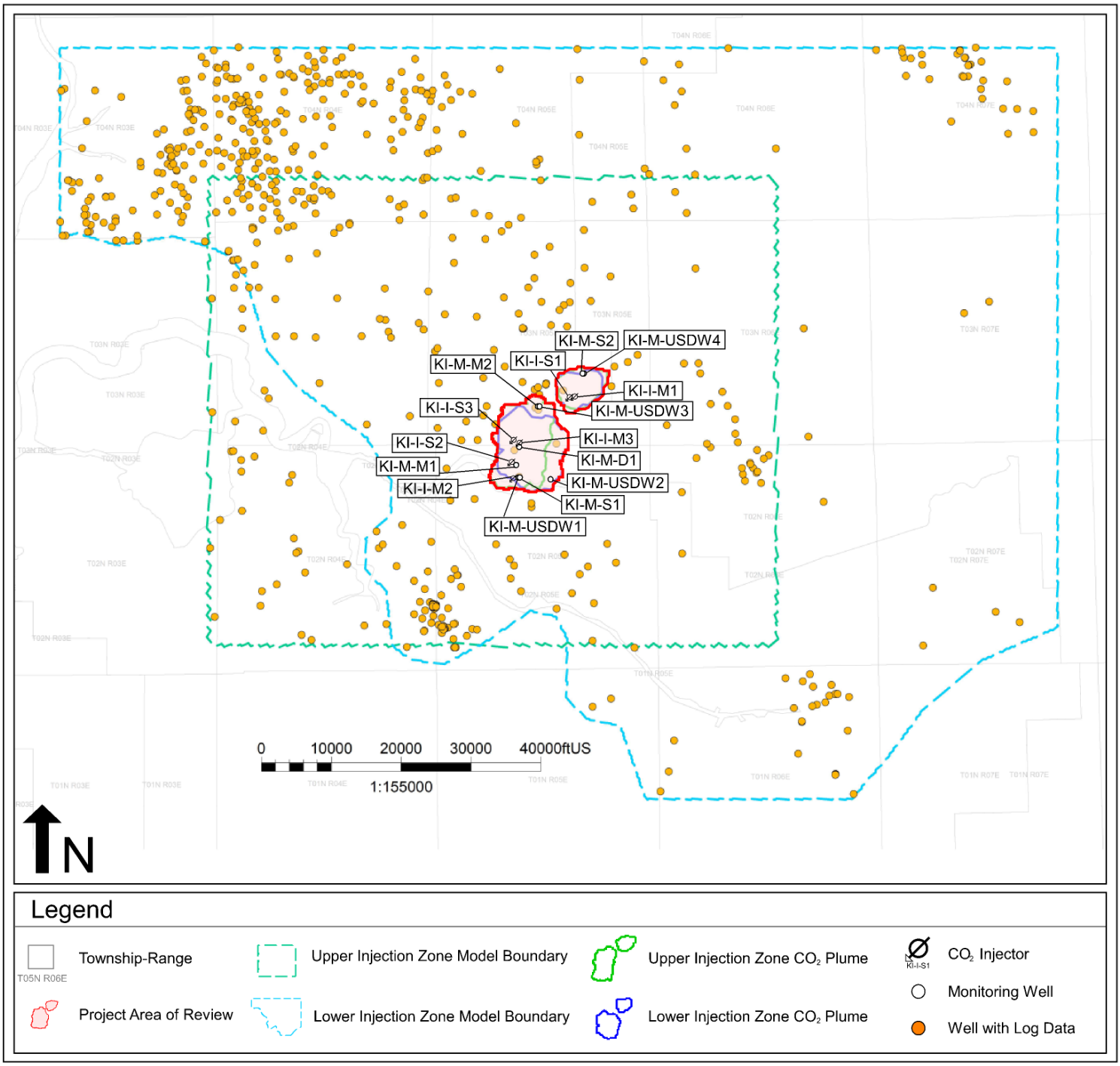

Figure 3.2. Location of wells with open-hole log data used to develop the static and computational models.

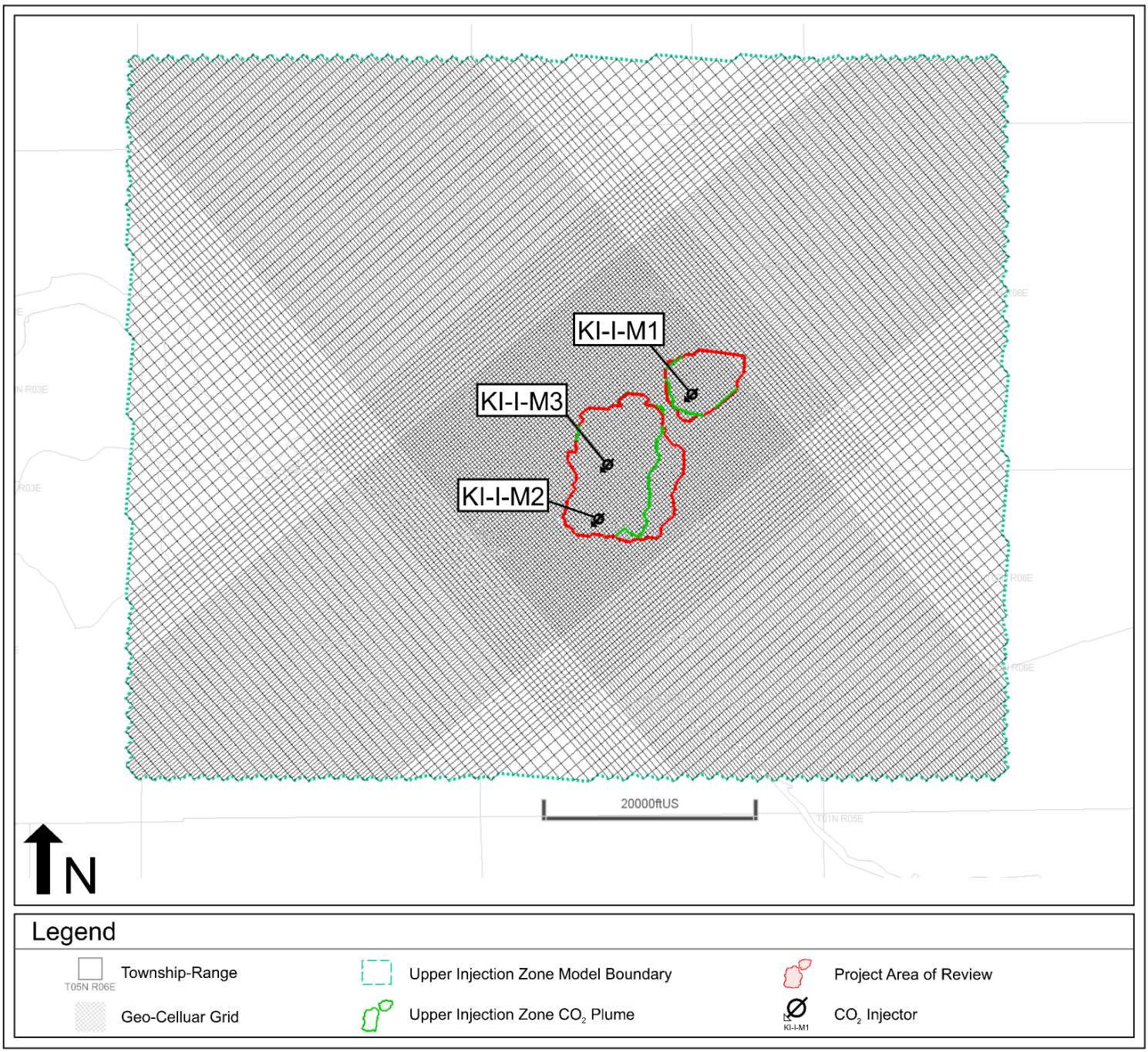

Figure 3.3a. Plan view of the Upper Injection Zone model boundary and geo-cellular grid used to define the CO_2 plume extent and associated project AoR.

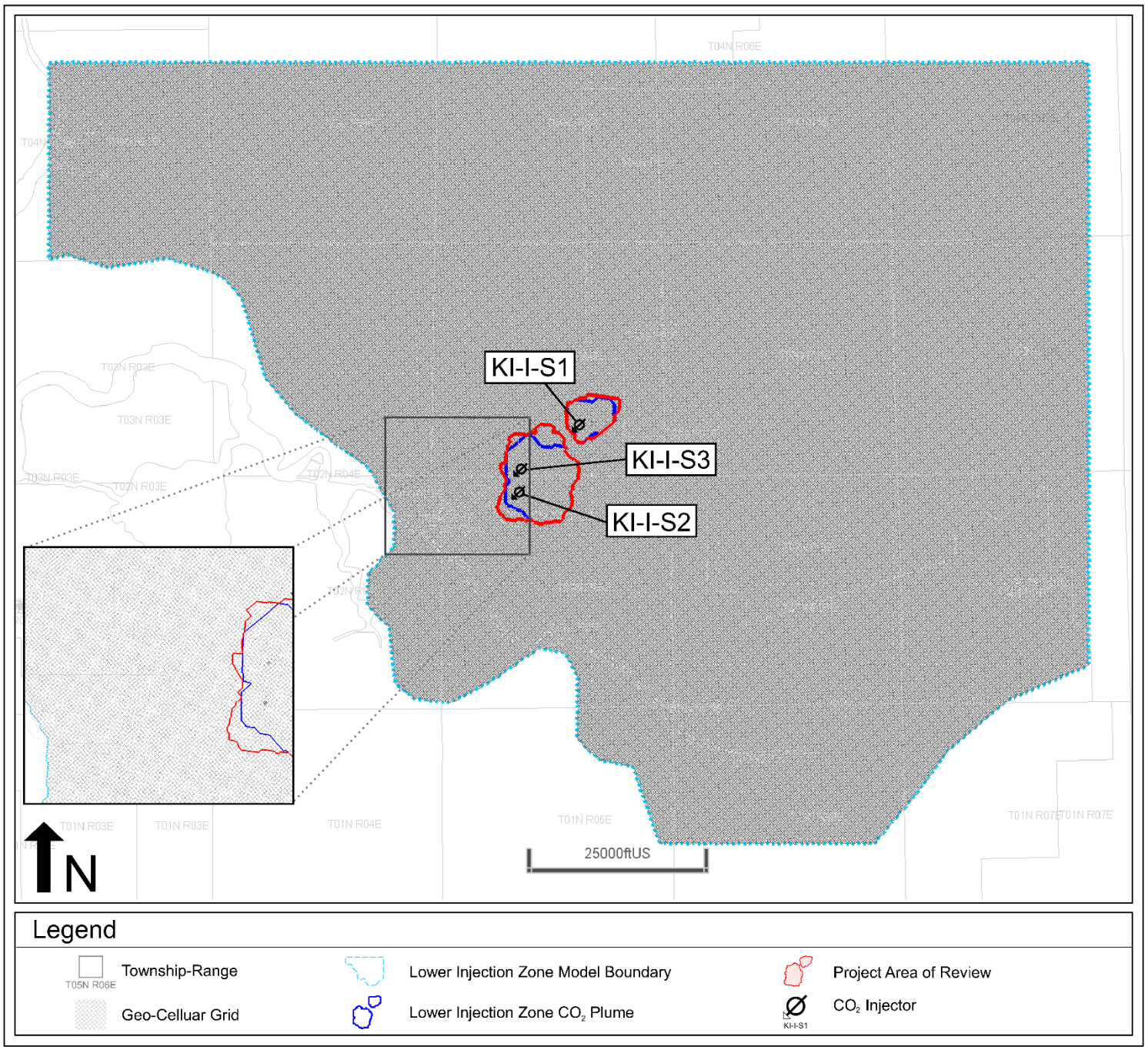

Figure 3.3b. Plan view of the Lower Injection Zone model boundary and geo-cellular grid used to define the CO_2 plume extent and associated project AoR.

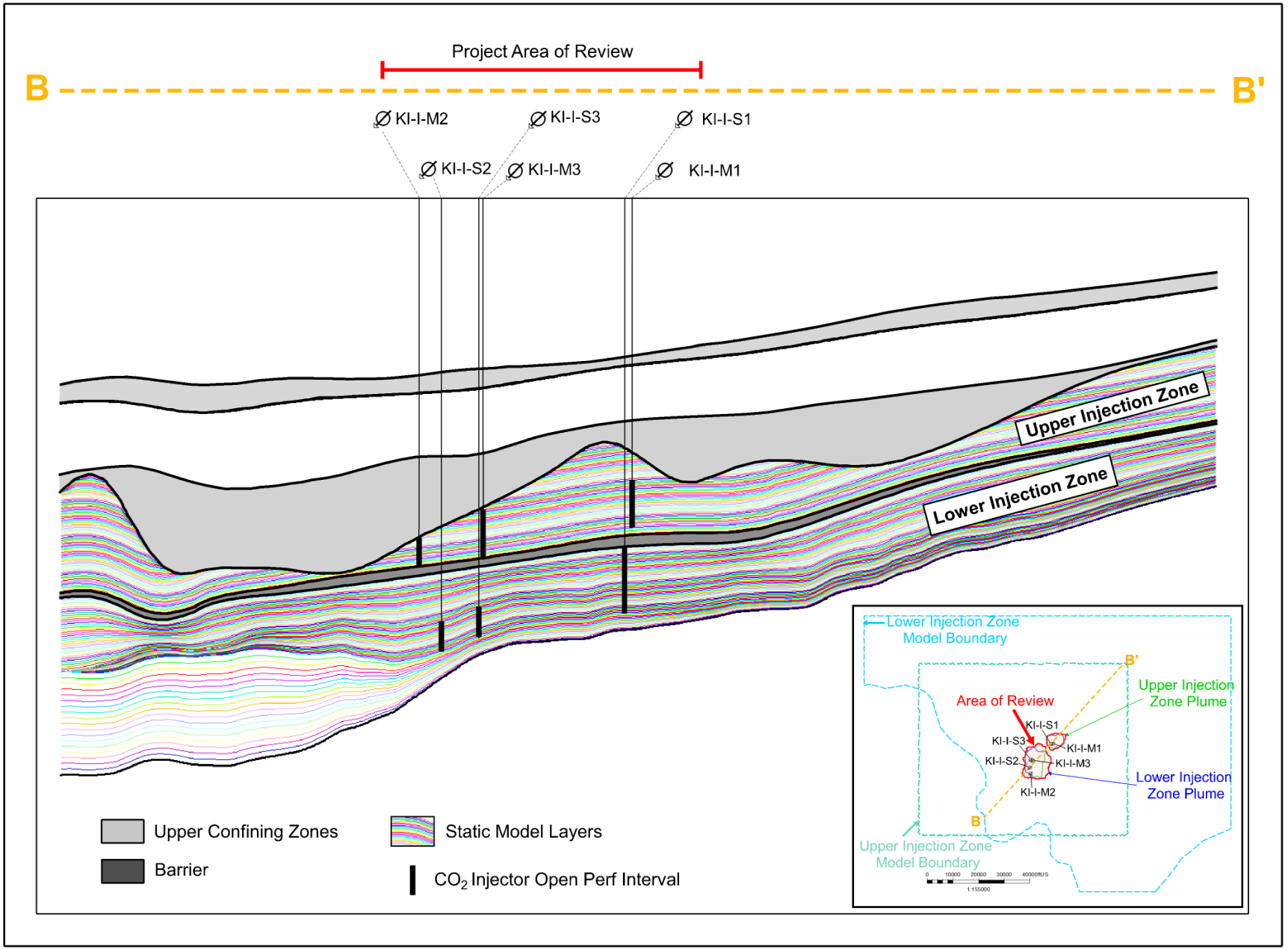

Figure 3.4. Static model grid layering of the Injection Zones. Stratigraphic units have an open boundary in all directions.

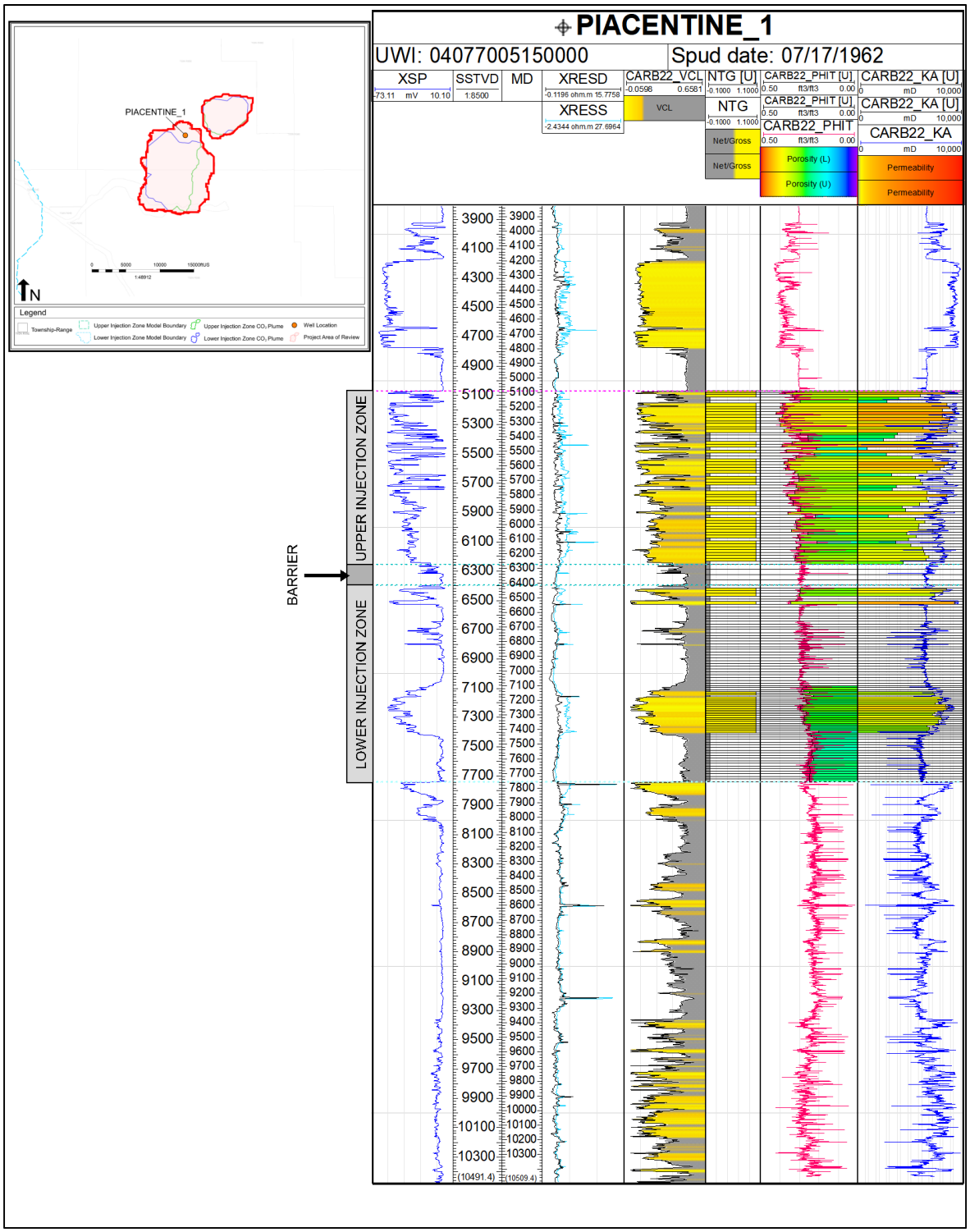

Figure 3.5. Well "PIACENTINE_1" upscaled logs versus open-hole logs.

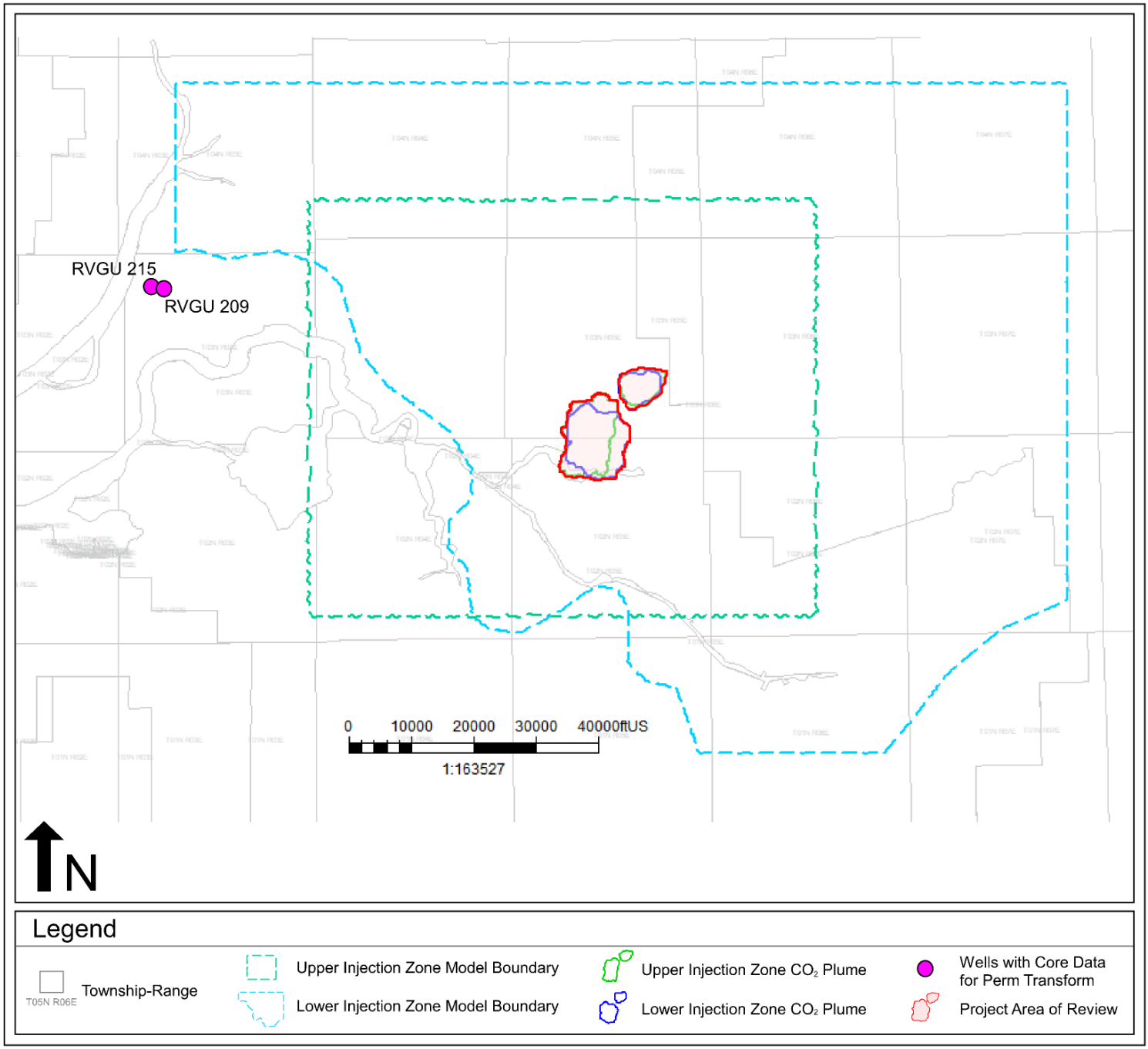

Figure 3.6: Location of wells with core data used for permeability transform.

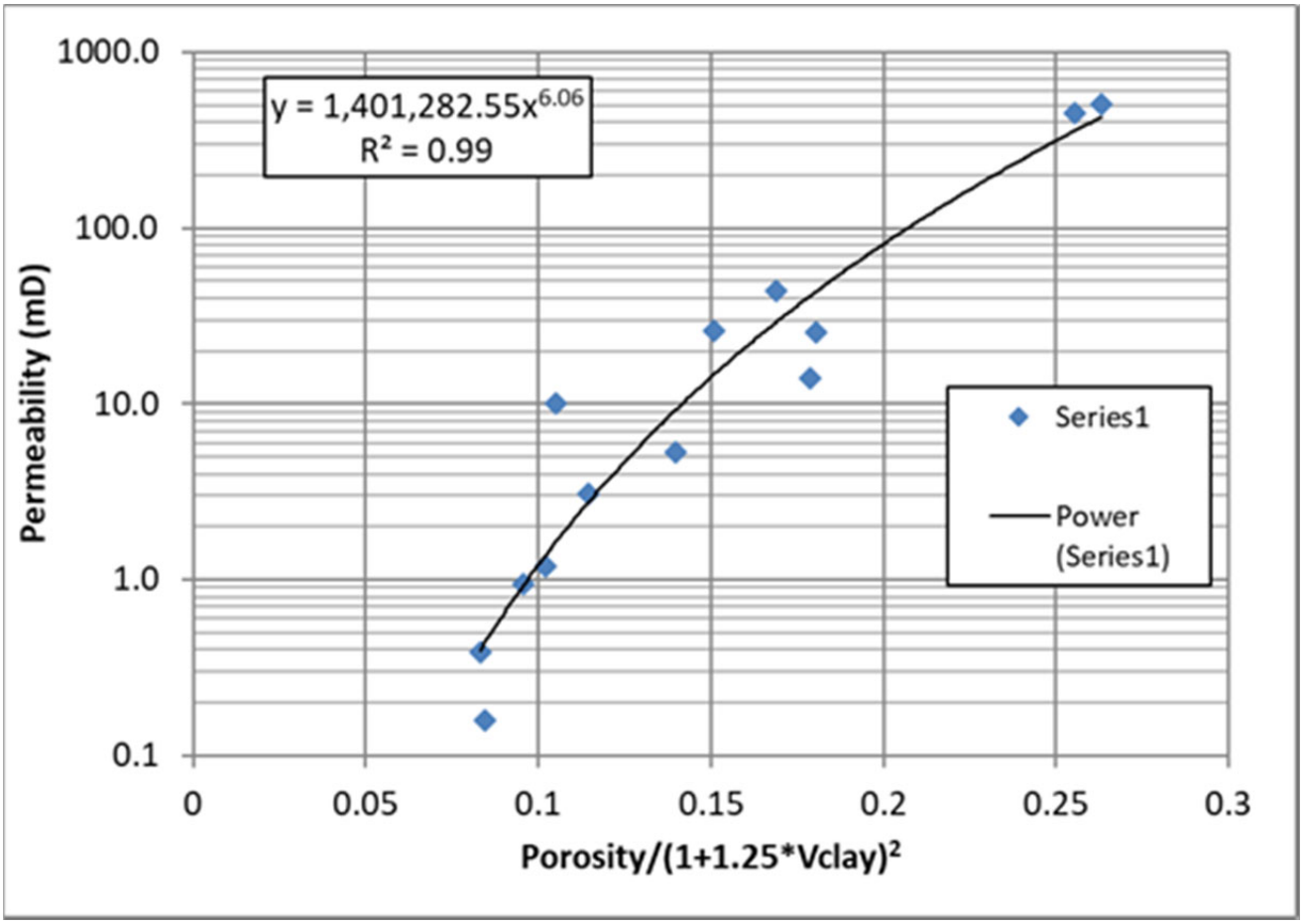

Figure 3.7: Permeability transform for Sacramento Basin zones

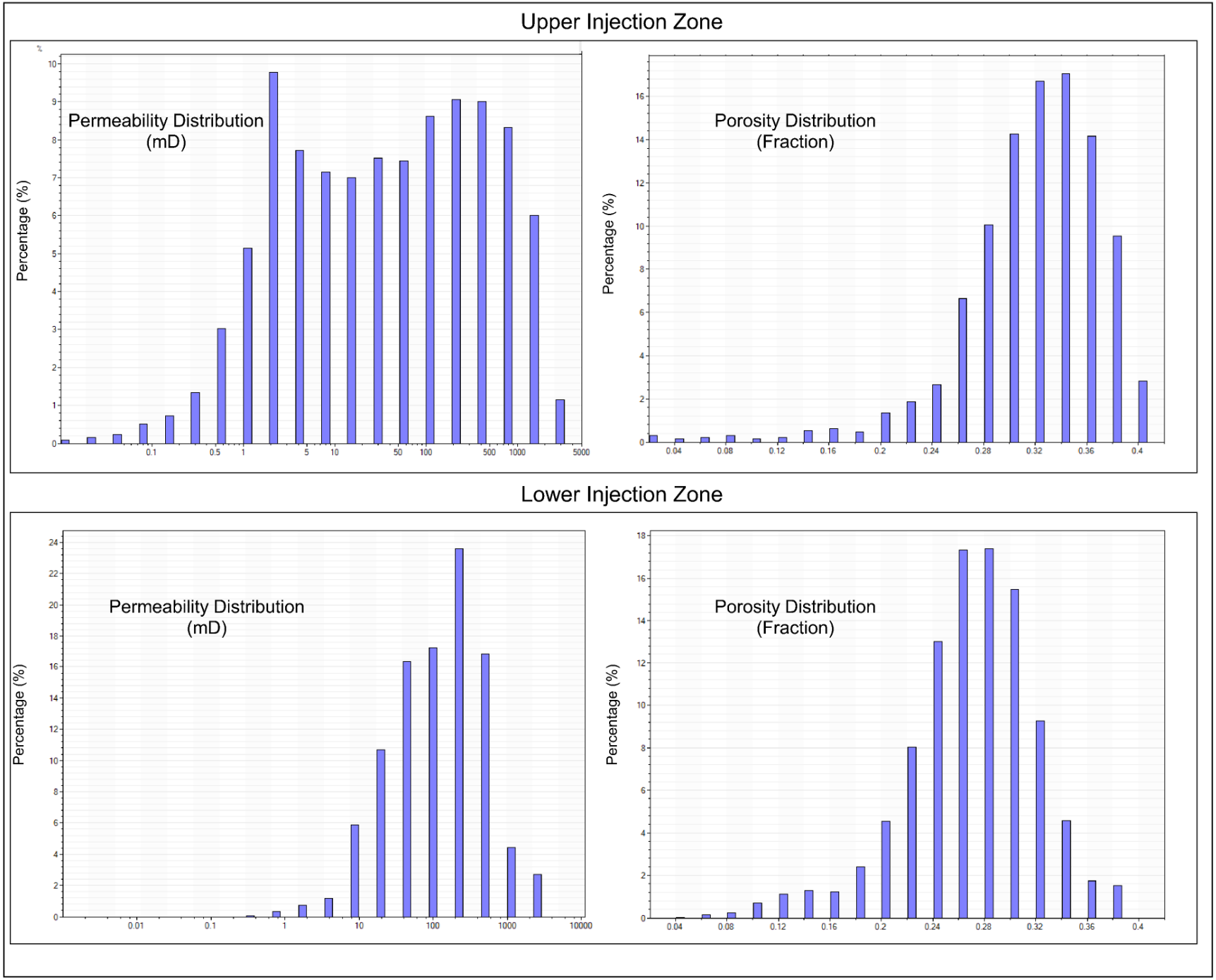

Figure 3.8. Upper and Lower Injection Zone porosity and permeability distribution used in the static model (excluding cells with net-to-gross equal to zero).

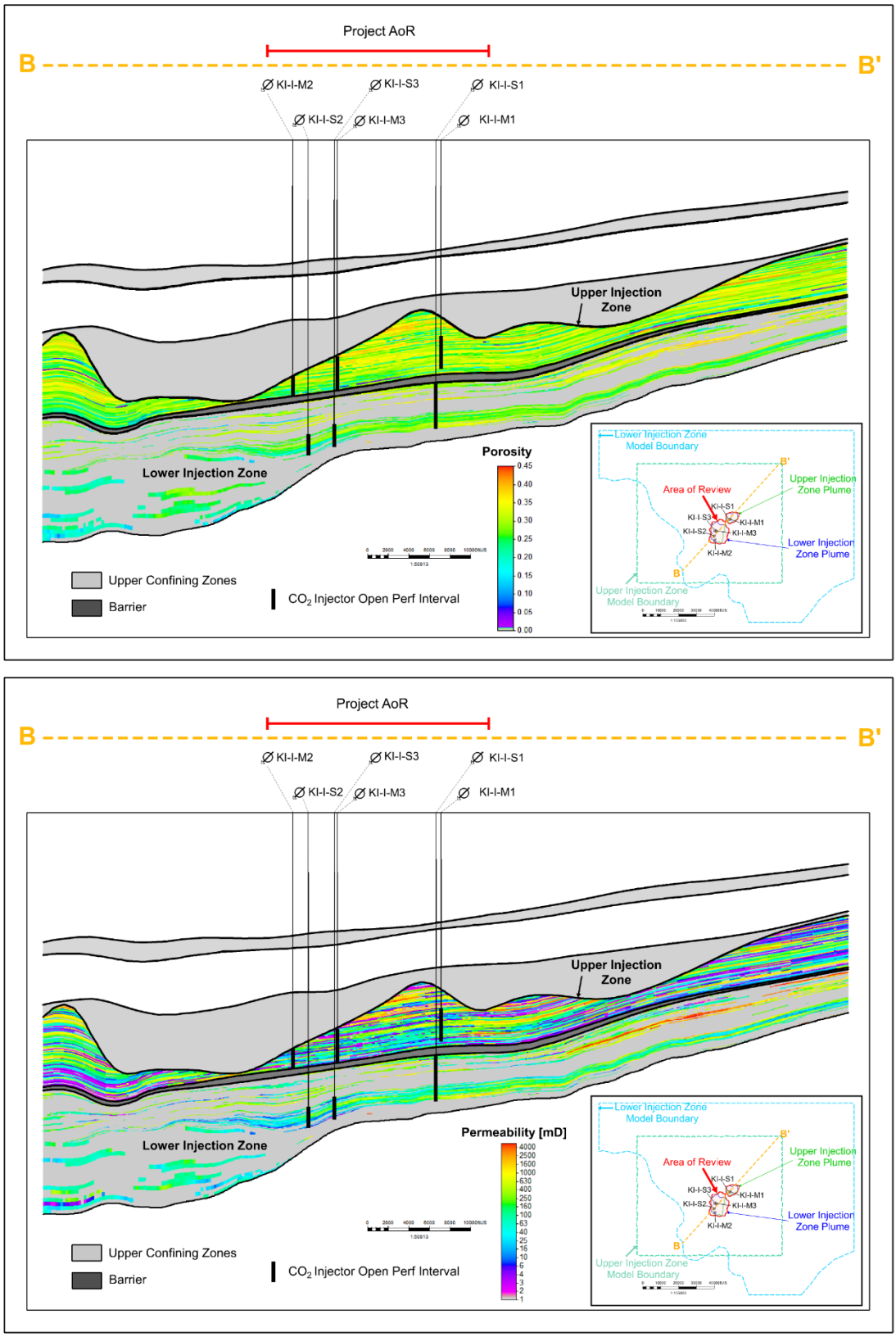

Figure 3.9. Sections through the static grid showing the distribution of porosity and permeability in the reservoir.

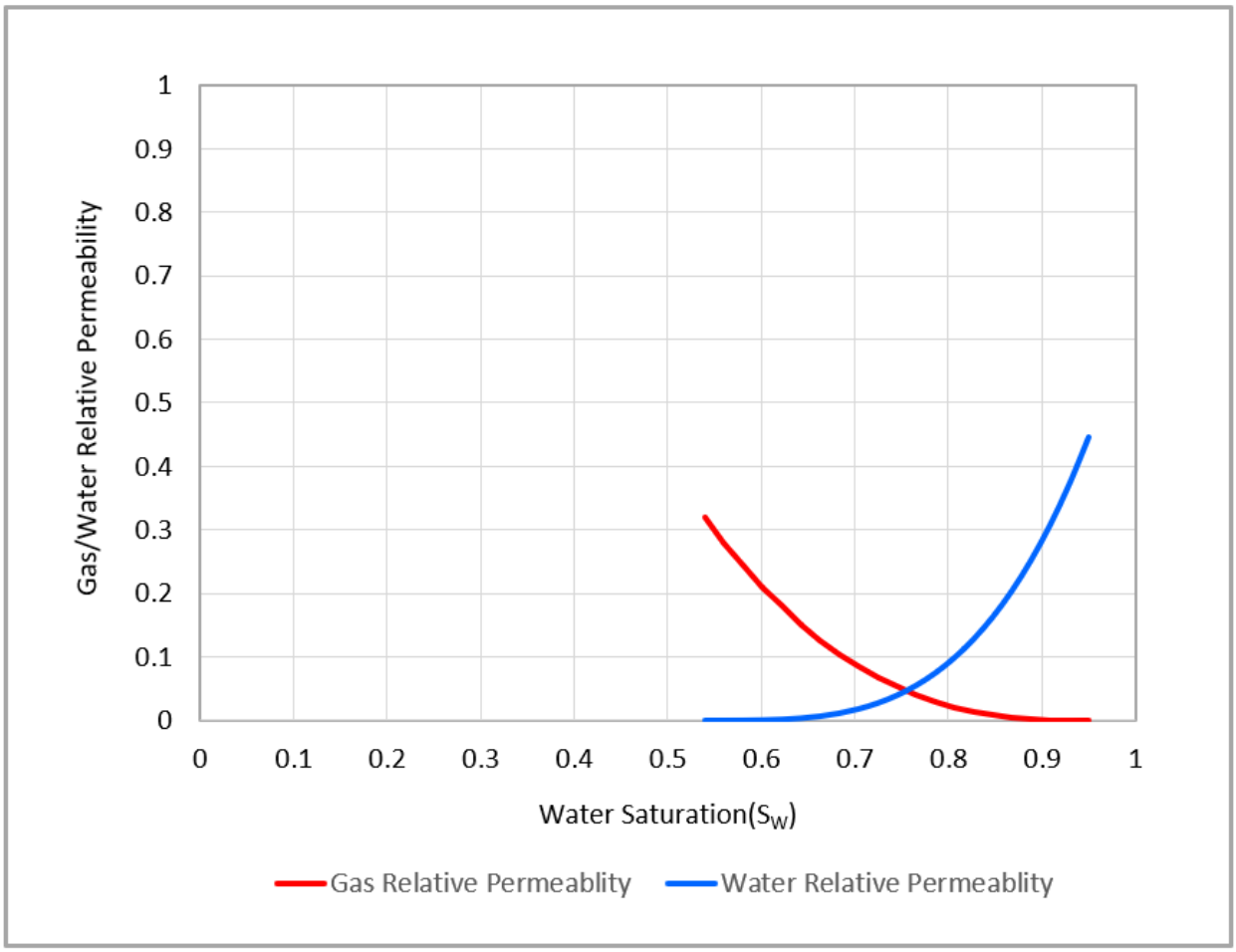

Figure 3.10. Relative permeability curves for Gas-Water system

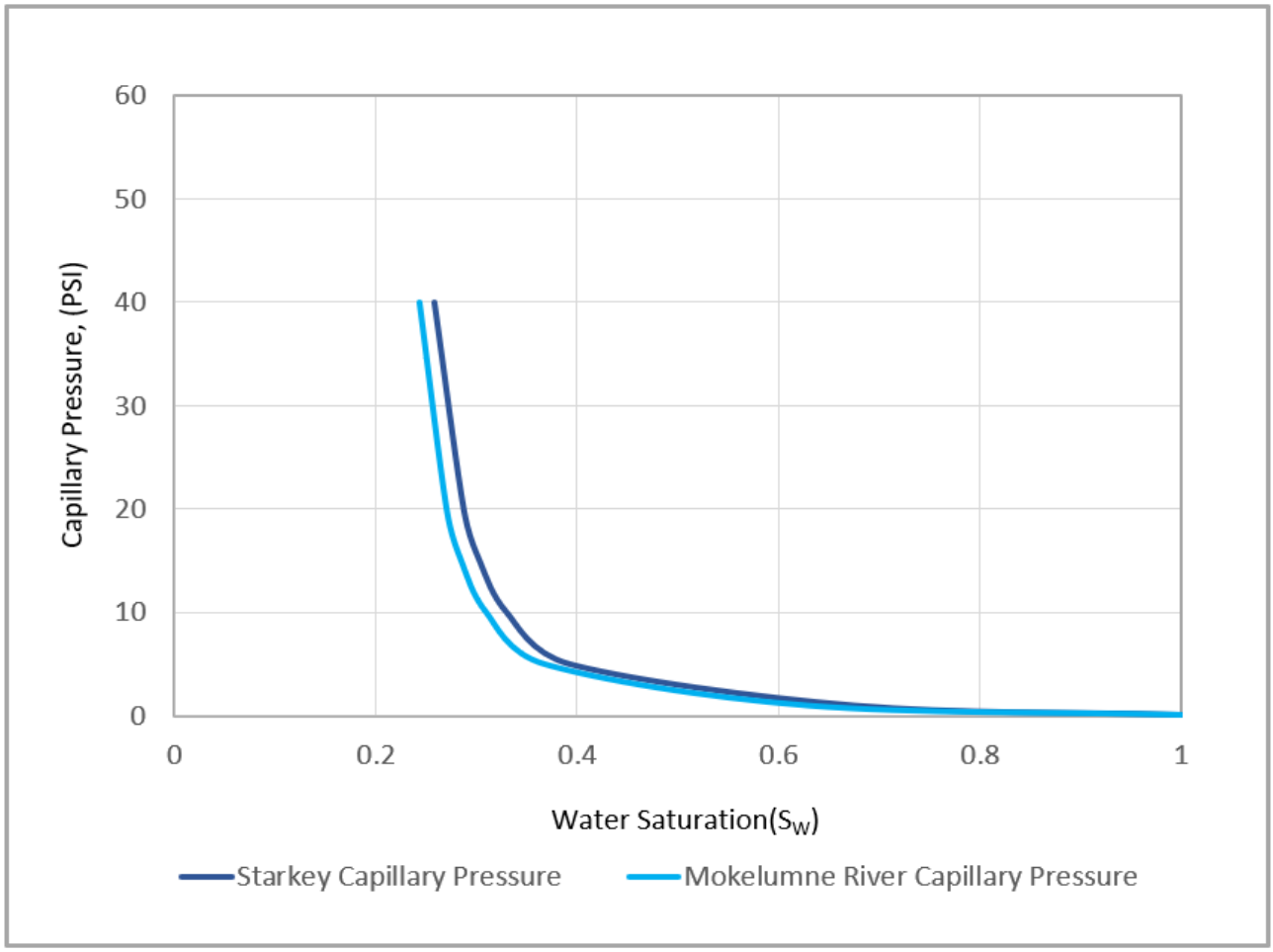

Figure 3.11. Capillary pressure curve

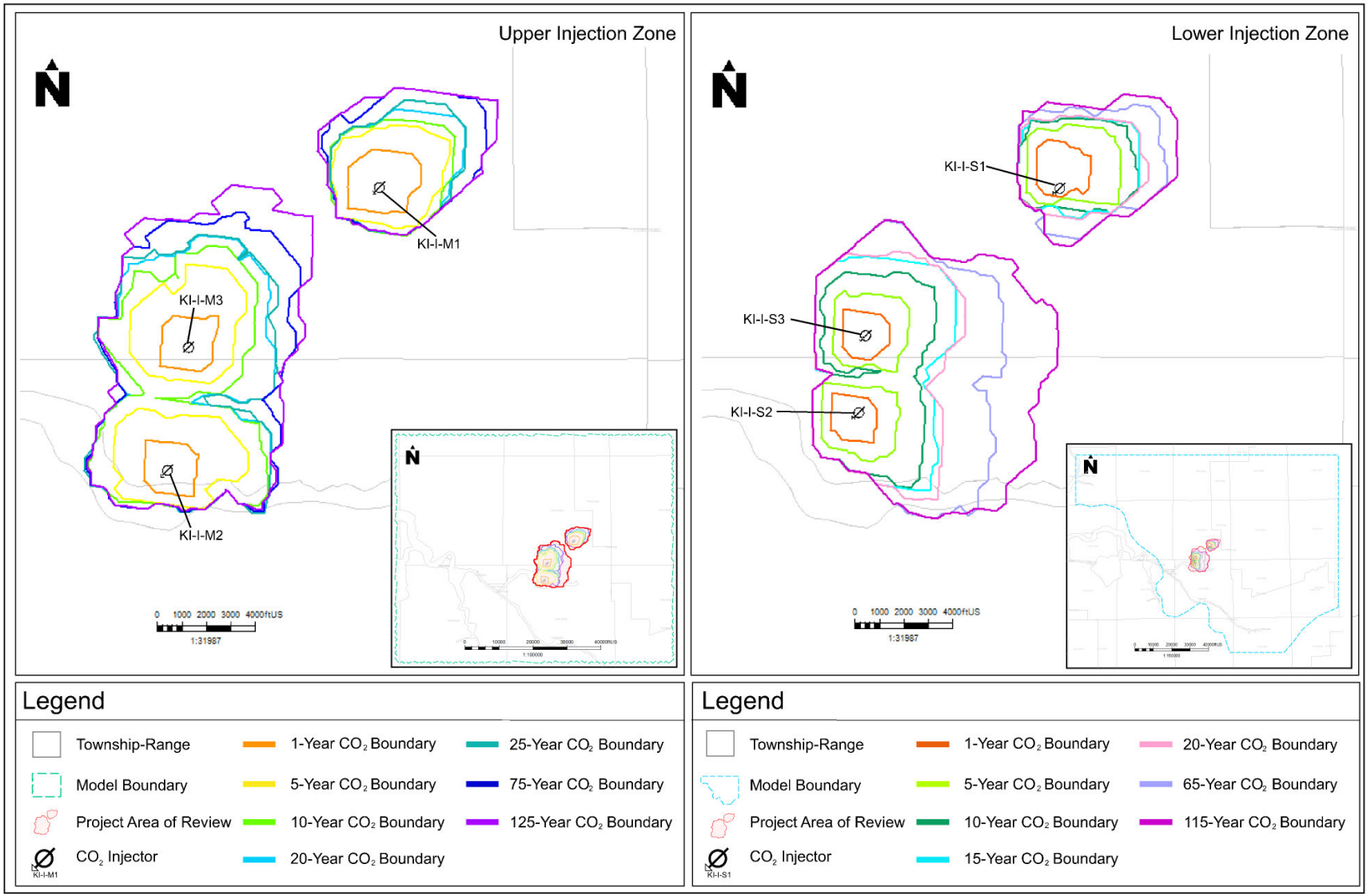

Figure 4.1 Upper Injection Zone plume development through time: 1-year, 5-year, 10-year, 15-year, 20-year, 25-year (end of injection), 50-year, and 100-year post injection (Left). Lower Injection Zone plume development through time: 1-year, 5-year, 10-year-, 15-year (end of injection), 5-year, 50-year, and 100-year post injection (Right).

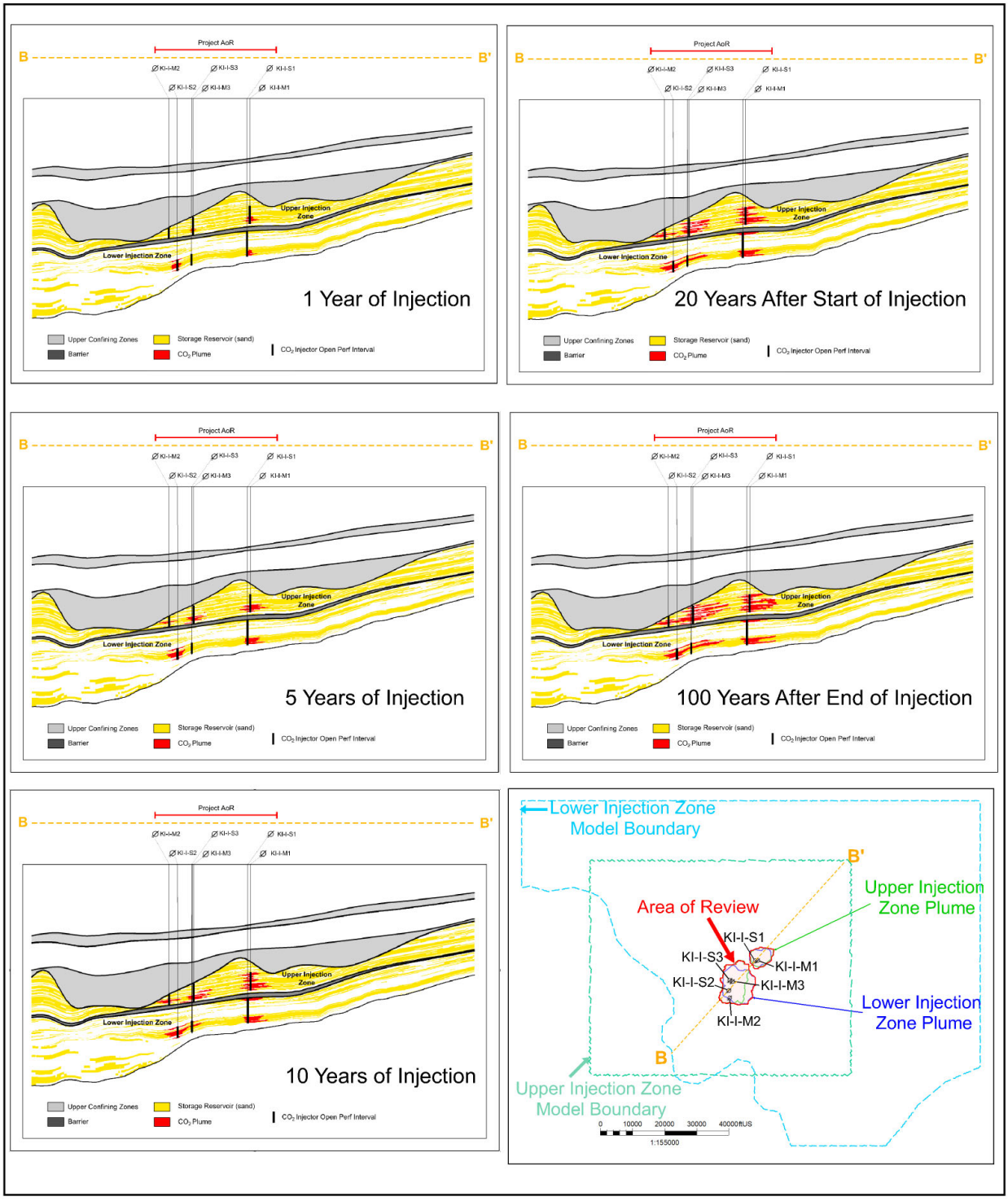

Figure 4.2 Cross-sections showing plume development at various time steps through the project

(A) Upper Injection Zone

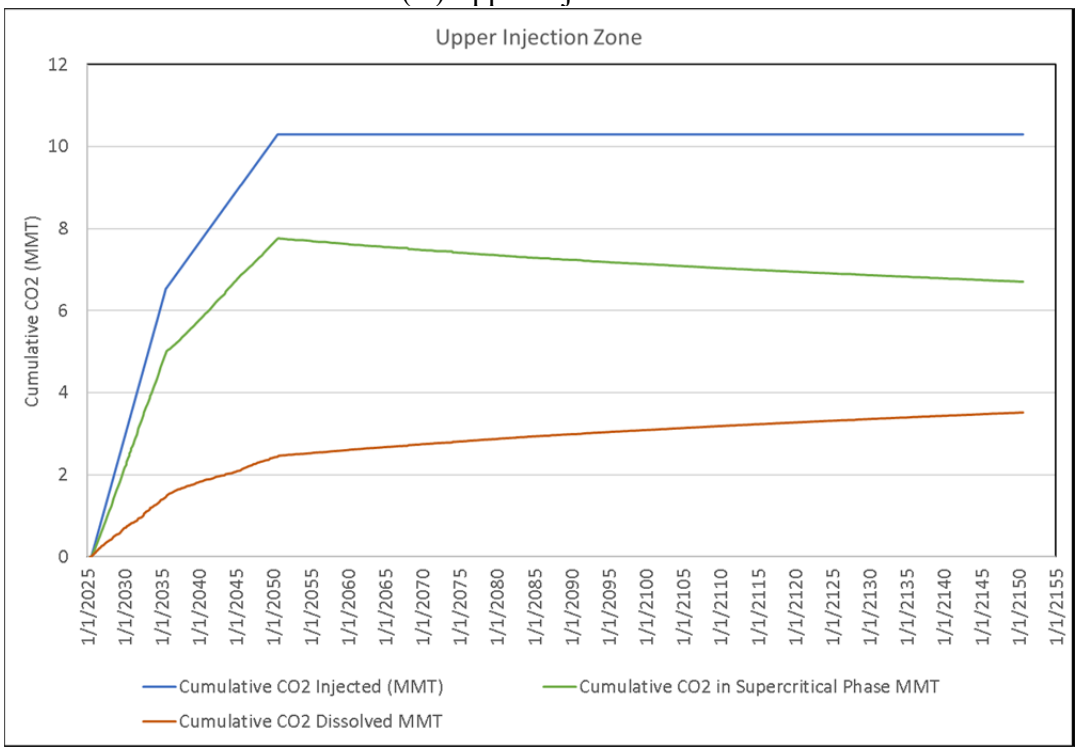

(B) Lower Injection Zone

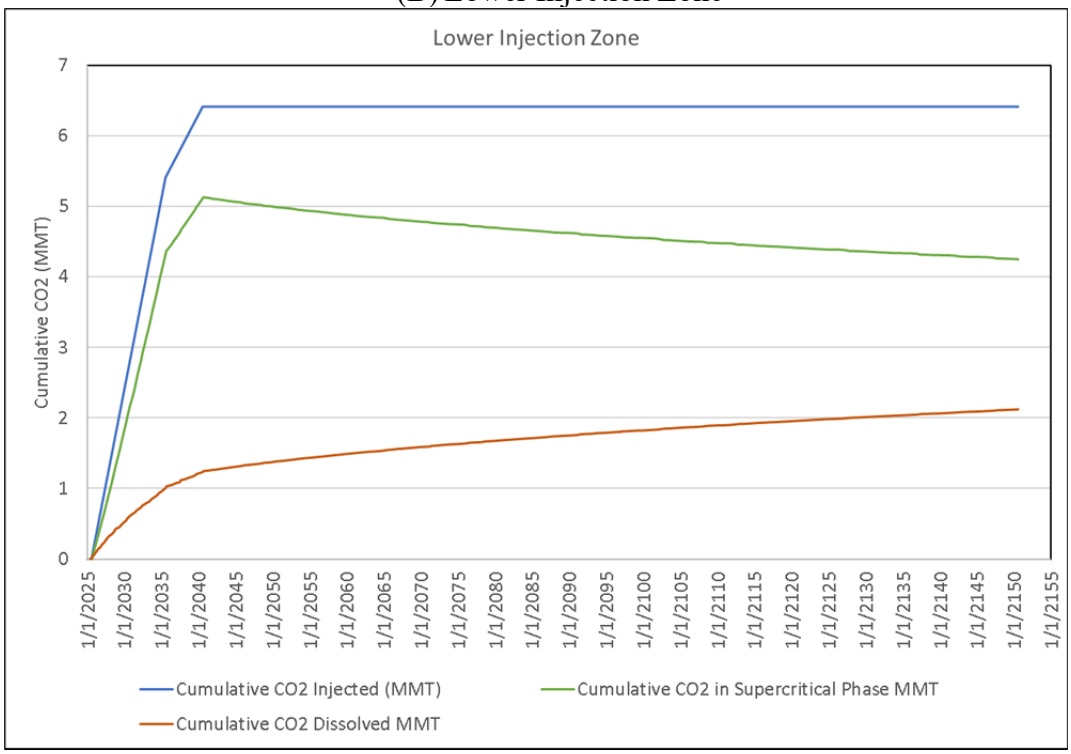

Figure 4.3 CO_2 storage mechanisms in the reservoir.

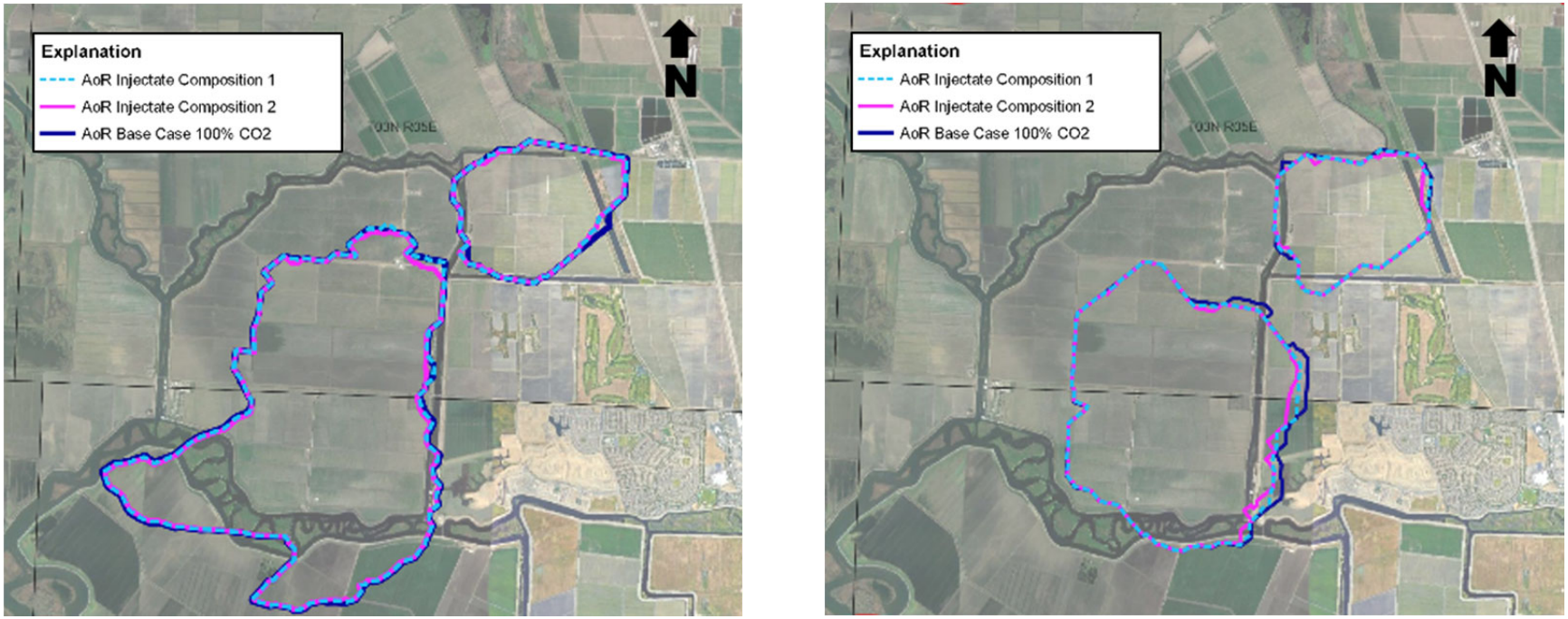

(A) Upper Injection Zone (B) Lower Injection Zone

Figure 4.4. AoR boundaries and CO_2 plume outlines for Injectate 1 (Light Blue), Injectate 2 (Pink) and 100% CO_2 Cases (Dark Blue). Minimal difference in AoR boundaries between the 3 cases with the boundaries overlying each other for the most part.

(A) Upper Injection Zone

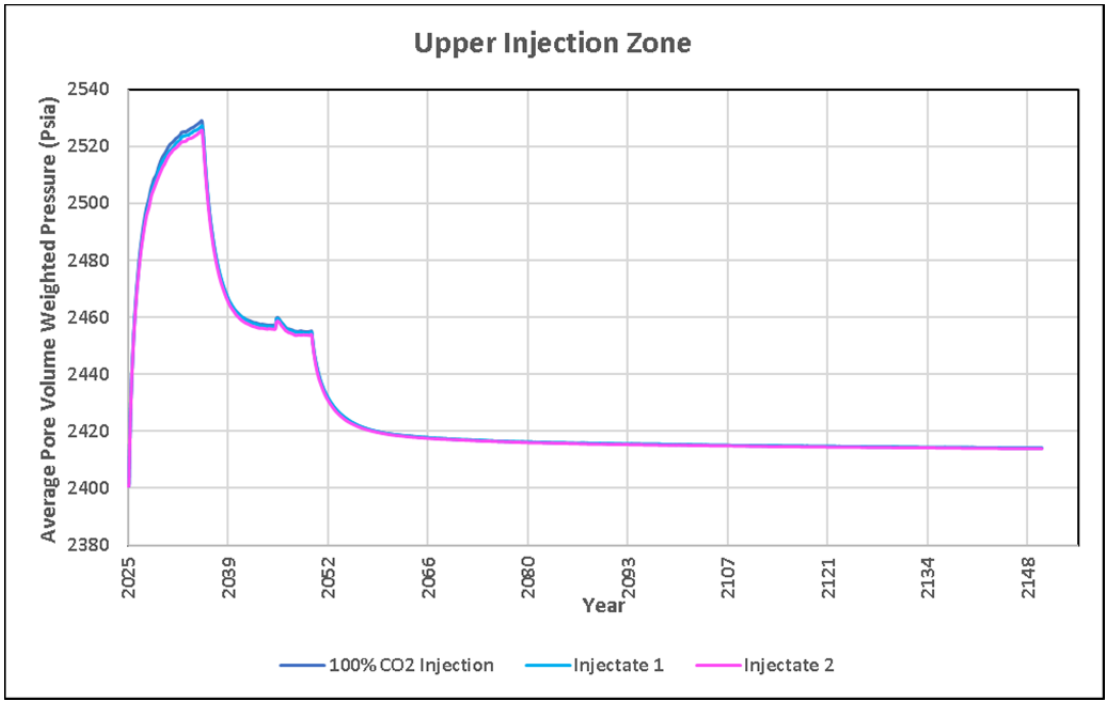

(B)Lower Injection Zone

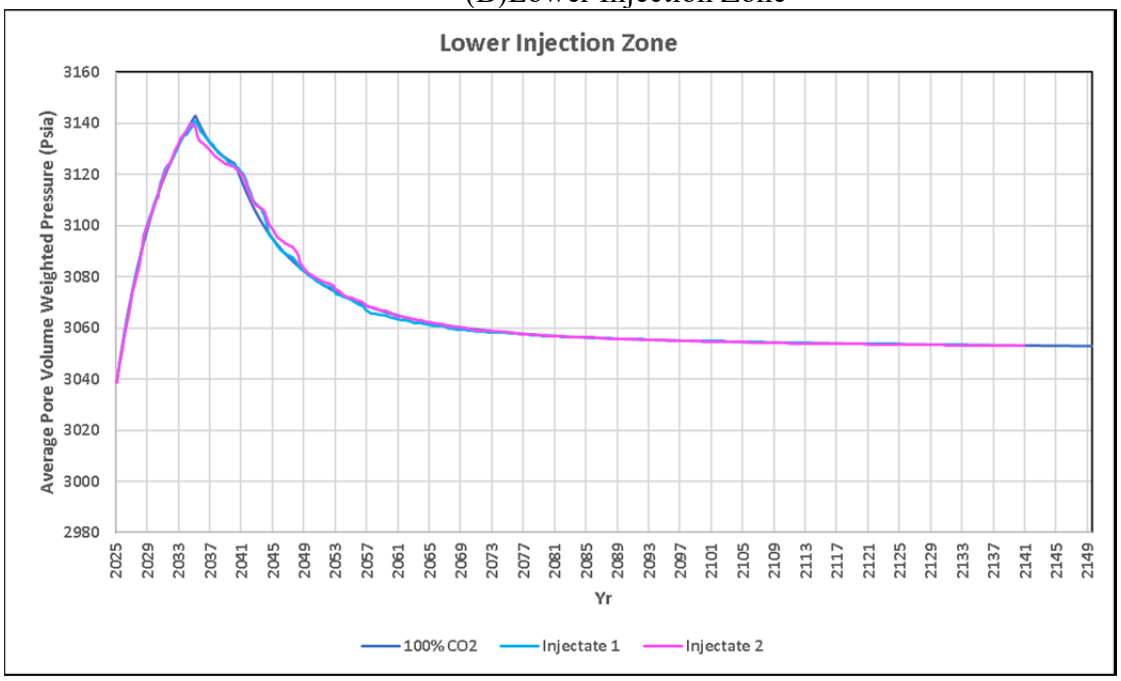

Figure 4.5. Average reservoir pressure within project vicinity for Injectate 1, Injectate 2 and 100% CO_2 cases. 100% CO_2 case and Injectate 2 case pressure trends plot almost on top of each other.

Well	Measured Depth TVD	Measured Res Press, psi	Pressure measurement method	Date measured
PGE Test Inj/withdrawal well 1	4,664	1,892	Formation test	10/19/2014
PGE Test Inj/withdrawal well 1	4,673	1,895	Formation test	10/19/2014
PGE Test Inj/withdrawal well 1	4,678	1,898	Formation test	10/19/2014
PGE Test Inj/withdrawal well 1	4,716	1,914	Formation test	10/19/2014
PGE Test Inj/withdrawal well 1	4,741	1,925	Formation test	10/19/2014
PGE Test Inj/withdrawal well 1	4,763	1,934	Formation test	10/19/2014
PGE Test Inj/withdrawal well 1	4,779	1,941	Formation test	10/19/2014
PGE Test Inj/withdrawal well 1	4,787	1,945	Formation test	10/19/2014
PGE Test Inj/withdrawal well 1	4,854	1,974	Formation test	10/19/2014
RVGU_198	4,857	1,663	Formation test	1/21/1996
RVGU_198	4,899	1,671	Formation test	1/21/1996
RVGU_198	4,912	1,673	Formation test	1/21/1996
RVGU_198	4,924	1,678	Formation test	1/21/1996
RVGU_198	4,957	1,729	Formation test	1/21/1996
McDonald Farms 9	5,270	1,960	Operator Pressure estimate	8/20/2016
PIACENTINE_2-27	4,695	1909	Formation test	3/25/2013
PIACENTINE_2-27	4,720	1920	Formation test	3/25/2013
PIACENTINE_2-27	4,754	1935	Formation test	3/25/2013
PIACENTINE_2-27	4,762	1938	Formation test	3/25/2013
PIACENTINE_2-27	4,774	1944	Formation test	3/25/2013
PIACENTINE_2-27	4,774	1943	Formation test	3/25/2013
PIACENTINE_2-27	4,788	1949	Formation test	3/25/2013
PIACENTINE_2-27	4,794	1952	Formation test	3/25/2013
PIACENTINE_2-27	4,804	1956	Formation test	3/25/2013
PIACENTINE_2-27	4,810	1959	Formation test	3/25/2013
STONE_LAKE_UNIT_1	5,074	2160	Formation test	10/11/2012

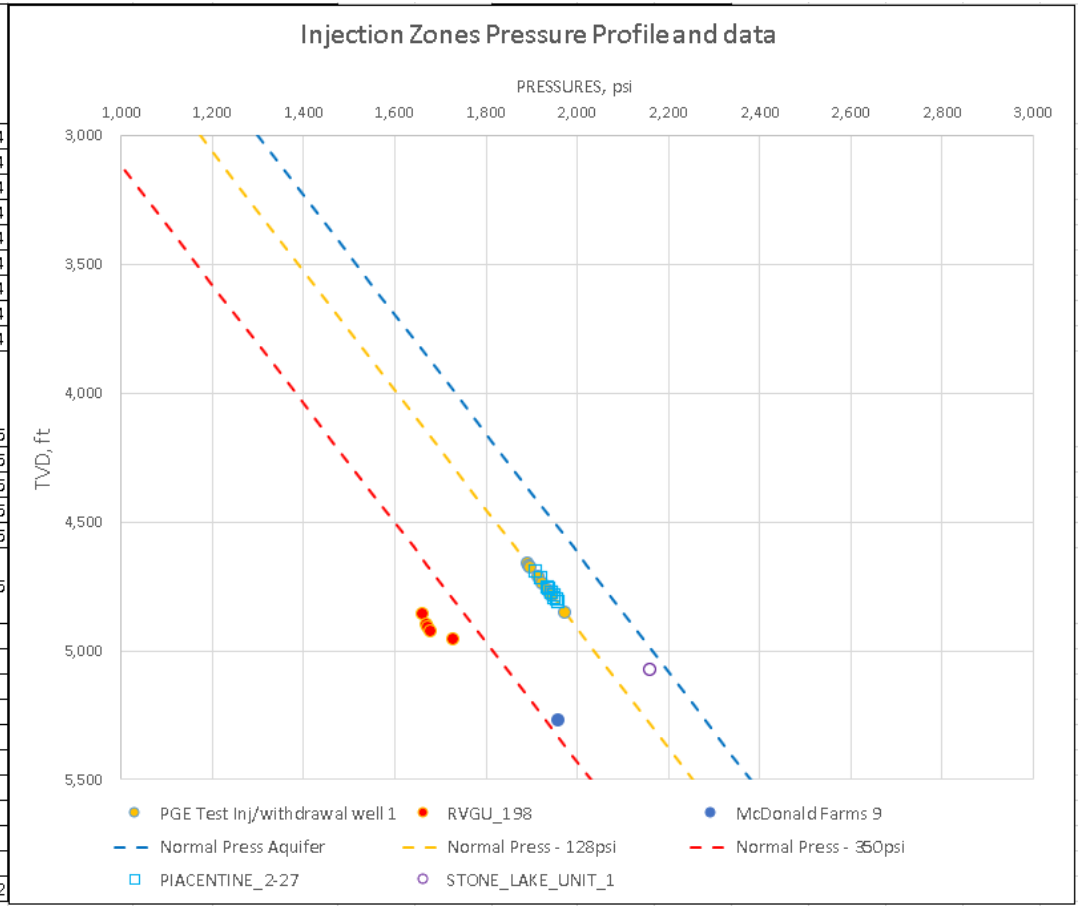

Figure 4.6. Upper Injection Zone pressure profile and data and Lower Injection Zone pressure profile and data.

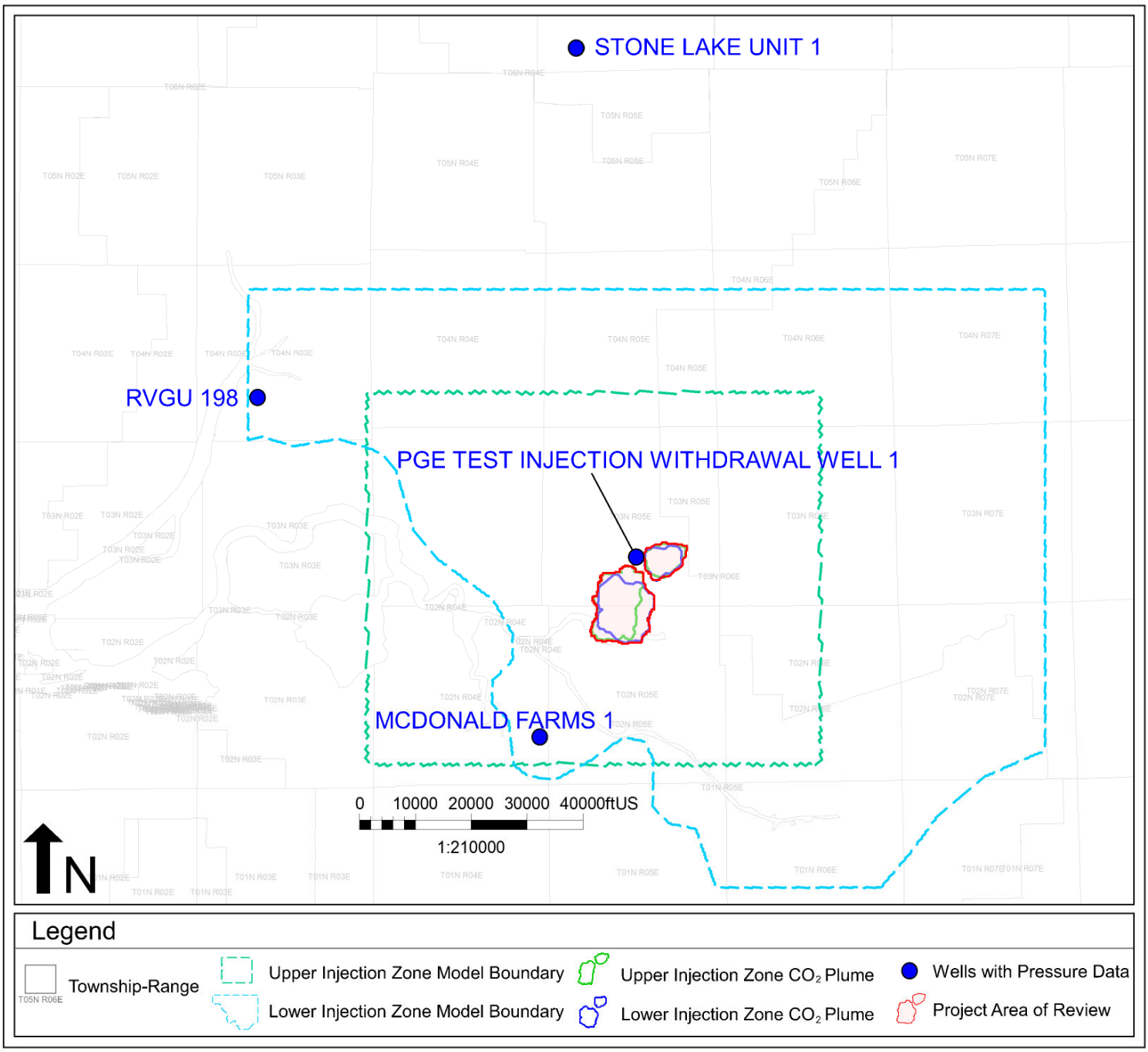

Figure 4.7. Map showing location of wells with pressure data for the Upper and Lower Injection Zones.

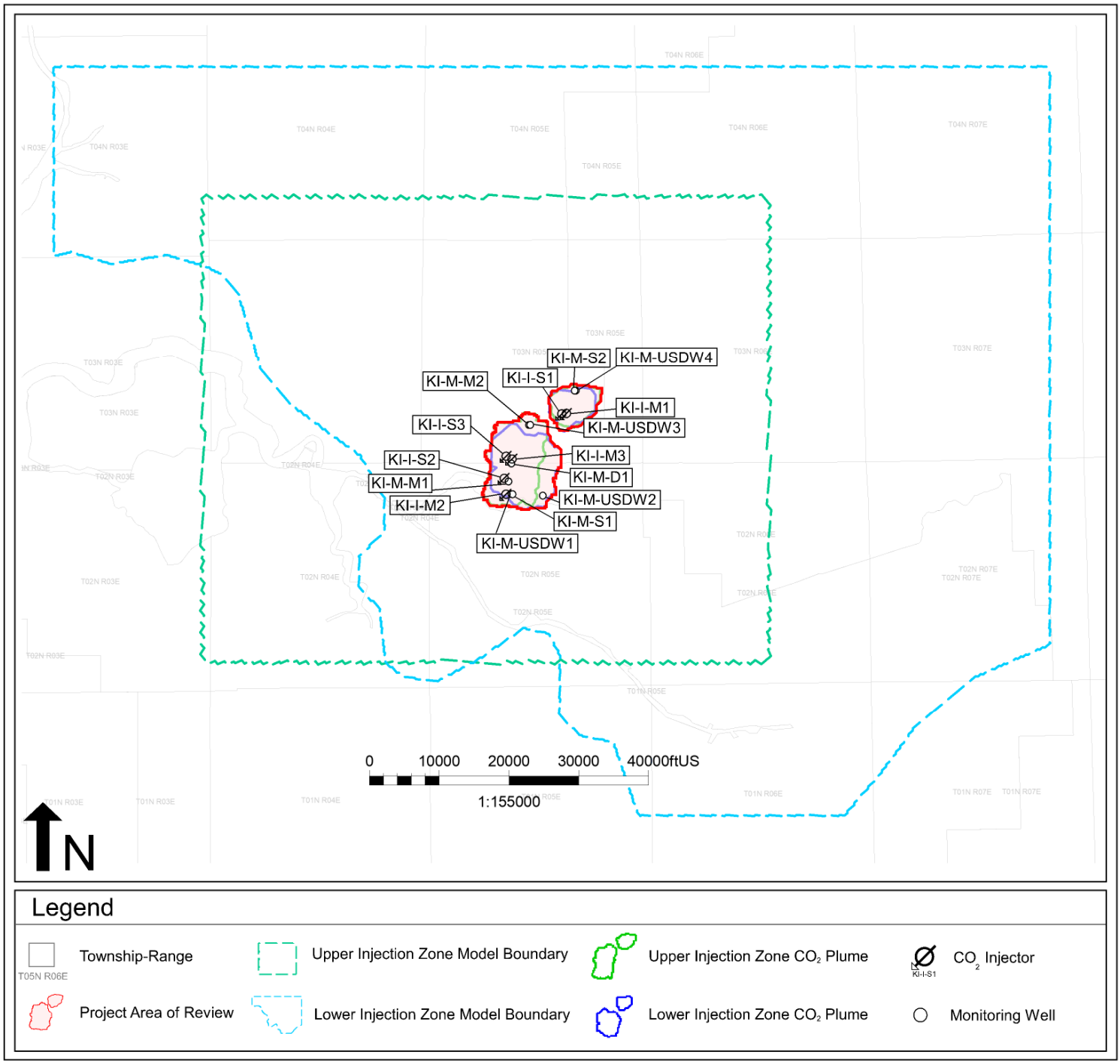

Figure 4.8. Map showing the location of injection and monitoring wells.

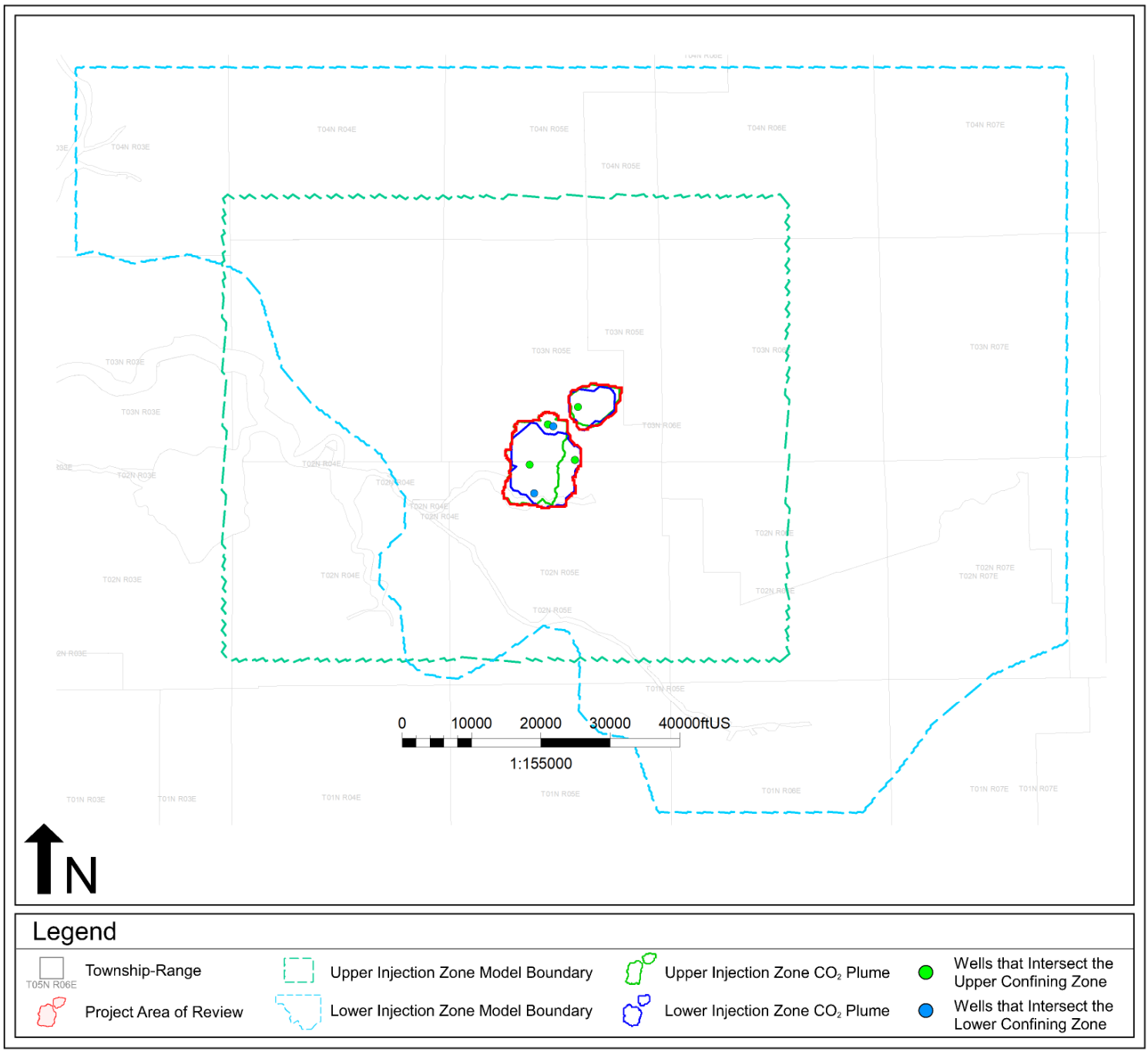

Figure 5.1. Wells penetrating the upper and lower confining layers and sequestration reservoirs in the AoR. Four wells are identified for corrective action at this time.

Tables

Table 3.1. Model domain information

a) Upper Injection Zone

Coordinate System	State Plane		
Horizontal Datum	North American Datum (NAD) 27		
Coordinate System Units	Feet		
Zone	Zone 2		
FIPSZONE	0402	**ADSZONE**	3301
Coordinate of X min	2,118,064.92	**Coordinate of X max**	2,199,975.99
Coordinate of Y min	114,200.90	**Coordinate of Y max**	181,655.35
Elevation of Bottom of Domain	-7657.58	**Elevation of Top of Domain**	-3,472.86

b) Lower Injection Zone

Coordinate System	State Plane		
Horizontal Datum	North American Datum (NAD) 27		
Coordinate System Units	Feet		
Zone	Zone 2		
FIPSZONE	0402	**ADSZONE**	3301
Coordinate of X min	2,097,000.31	**Coordinate of X max**	2,239,999.39
Coordinate of Y min	92,453.63	**Coordinate of Y max**	199,999.69
Elevation of Bottom of Domain	-9842.49	**Elevation of Top of Domain**	-2351.80

Table 3.2. Sonic porosity equations by zone

Zones	Sonic Porosity Equation	Wyllie Compaction Factor
Nortonville Shale-Domengine	Wyllie	1.3
Capay Shale – Mokelumne River Formation	Wyllie	1.2
H&T Shale-Sawtooth Shale	Wyllie	1.0

Table 3.3. Initial conditions

Parameter	Injection Zone	Value	Units	Corresponding Elevation (ft msl)	Data Source
Temperature	Lower	152°	Fahrenheit	7,000	Bottom hole temperature data from logs in area
	Upper	136°		5,800	
Formation Pressure	Lower	2,994	Pounds per square inch	7,000	37 psi below hydrostatic based on offset field production
	Upper	2,383		5,800	128 psi below hydrostatic based on offset field production
Salinity	Lower	14,000	Parts per million	7,000	Water analysis and log calculated salinity curves
	Upper	14,000		5,800	

Table 3.4. Operational details

Operating Information	Injection Well KI-I-M1 Upper Zone	Injection Well KI-I-M2 Upper Zone	Injection Well KI-I-M3 Upper Zone	Injection Well KI-I-S1 Lower Zone	Injection Well KI-I-S2 Lower Zone	Injection Well KI-I-S3 Lower Zone
Location: Latitude, Longitude	38.07744211, -121.40743930	38.04576610, -121.437838	38.05957602, -121.434721	38.07718008, -121.409794	38.05202188, -121.438679	38.06072103, -121.437648
Model coordinates (ft) X, Y	2170589.37, 150158.73	2161909.31, 138567.48	2162775.75, 143602.30	2169912.04, 150058.90	2161653.05, 140844.19	2161930.30, 144014.06
No. of perforated intervals	3	1	3	2	2	3
Perforated interval (ft MD/TVD/MSL) Top, Bottom	5,423/5,419/5,400, 6,041/6,036/6,017	6,456/6,399/6,380, 6,658/6,599/6,580	5,827/5,801/5,782, /6,491/6,460/6,441	6,421/6,302/6,283, 7,369/7,221/7,202	7,404/7,336/7,317, 7,812/7,738/7,719	7,198/6,958/6,939, 7,795/7,554/7,535
Casing diameter (in.)	7	7	7	7	7	7
Modeled injection period Start End	08/01/2025 08/01/2035	08/01/2025 08/01/2035	08/01/2025 08/01/2050	08/01/2025 08/01/2035	08/01/2025 08/01/2035	08/01/2025 08/01/2040
Modeled Injection duration (years)	10	10	25	10	10	15
Modeled Injection rate (KTons/year)*	250	150	250	190	150	200
Modeled CO_2 Injected (MMT)	2.52	1.5	6.273	1.91	1.502	3.0

*If planned injection rates change year to year, add rows to reflect this difference, and include an average injection rate per year (or interval if applicable).

Table 3.5. Injection pressure details

Injection Pressure Details	Injection Well KI-I-M1 Upper Zone	Injection Well KI-I-M2 Upper Zone	Injection Well KI-I-M3 Upper Zone	Injection Well KI-I-S1 Lower Zone	Injection Well KI-I-S2 Lower Zone	Injection Well KI-I-S3 Lower Zone
Fracture gradient (psi/ft)	0.76	0.76	0.76	0.76	0.76	0.76
Maximum allowable downhole injection pressure (90% of fracture pressure) (psi)	3,707	4,377	3,968	4,311	5,018	4,759
Elevation corresponding to maximum injection pressure (ft TVD)	5,419	6,399	5,801	6,302	7,336	6,958
Elevation at the top of the perforated interval (ft TVD)	5,419	6,399	5,801	6,302	7,336	6,958
Planned injection pressure (psi) / gradient (psi/ft) at top of perforations	2,395 / 0.44	2,887 / 0.45	2,903 / 0.5	2,911 / 0.46	3,348 / 0.46	3,205 / 0.46

Table 4.1. Simulation sensitivity scenarios

Scenario	CO_2 plume and AoR impact
Porosity: 10% reduction from base case	Minimal Impact
Porosity: 10% increase from base case	Minimal Impact
Permeability: 10% reduction from base case	Minimal Impact
Permeability: 10% increase from base case	Minimal Impact

Table 5.1. Wellbores in the AoR by status

Status	Count
Active	0
Idle	0
Plugged and Abandoned	6
Total	**6**